UNICAMP

UNIVERSIDADE ESTADUAL DE CAMPINAS

Instituto de Biologia

MARIELI MARIANO GONÇALVES DIAS

EXPLORANDO A MODULAÇAO DO PPARγ A PARTIR DA FOSFORILAÇÃO DA S273

Campinas

2024

MARIELI MARIANO GONÇALVES DIAS

EXPLORANDO A MODULAÇAO DO PPARγ A PARTIR DA FOSFORILAÇÃO DA S273

Tese apresentada ao Instituto de Biologia da Universidade Estadual de Campinas como parte dos requisitos exigidos para a obtenção do título de Doutora em Biologia Molecular e Morfofuncional na Àrea de Bioquimica.

Supervisor/Orientador: Ana Carolina Migliorini Figueira

ESTE TRABALHO CORRESPONDE À VERSÃO FINAL DA TESE DEFENDIDA PELO ALUNO MARIELI MARIANO GONÇALVES DIAS, E ORIENTADA PELA PROFA. DRA. ANA CAROLINA MIGLIORINI FIGUEIRA.

Campinas

2024

Ficha catalográfica
Universidade Estadual de Campinas (UNICAMP)
Biblioteca do Instituto de Biologia
Mara Janaina de Oliveira - CRB 8/6972

D543e

Dias, Marieli Mariano Gonçalves, 1990-
Explorando a modulação do PPARy a partir da fosforilação da S273 / Marieli Mariano Gonçalves Dias. – Campinas, SP : [s.n.], 2024.

Orientador(es): Ana Carolina Migliorini Figueira.
Tese (doutorado) – Universidade Estadual de Campinas (UNICAMP), Instituto de Biologia.

1. PPAR gama. 2. Fosforilação. 3. Serina. 4. Obesidade. I. Figueira, Ana Carolina Migliorini, 1980-. II. Universidade Estadual de Campinas (UNICAMP). Instituto de Biologia. III. Título.

Informações complementares

Título em outro idioma: Exploring the modulation of PPARy through phosphorylation of S273
Palavras-chave em inglês:
PPAR gamma
Phosphorylation
Serine
Obesity
Área de concentração: Bioquímica
Titulação: Doutora em Biologia Molecular e Morfofuncional
Banca examinadora:
Ana Carolina Migliorini Figueira [Orientador]
Deborah Schechtman
Alessandro Silva Nascimento
Leonardo dos Reis Silveira
Fernando Alves de Melo
Data de defesa: 09-12-2024
Programa de Pós-Graduação: Biologia Molecular e Morfofuncional

Identificação e informações acadêmicas do(a) aluno(a)
- ORCID do autor: https://orcid.org/0000-0002-0246-8884
- Currículo Lattes do autor: http://lattes.cnpq.br/1337169632103126

Campinas, 09 de dezembro de 2042

COMISSÃO EXAMINADORA

Profa. Dra. Ana Carolina Migliorini Figueira

Dra. Deborah Schechtman

Dr. Alessando Silva Nascimento

Dr. Fernando Alves de Melo

Prof.Dr. Leonardo dos Reis Silveira

Os membros da Comissão Examinadora acima assinaram a Ata de Defesa, que se encontra no processo de vida acadêmica do aluno.

A Ata da defesa com as respectivas assinaturas dos membros encontra-se no SIGA/Sistema de Fluxo de Dissertação/Tese e na Secretaria do Programa (inserir o nome do programa de pós) da Unidade (inserir o nome da faculdade/instituto).

AGRADECIMENTOS

A todos aqueles que caminharam ao meu lado durante essa jornada, seja por pouco ou muito tempo. Aqueles que estão comigo desde o começo e aqueles que acabaram de chegar. Todos vocês contribuíram um pouquinho para que essa etapa fosse cumprida.

À minha orientadora, Drª Ana Carolina Figueira, agradeço a oportunidade, paciência e disponibilidade para inúmeras discussões, além de todo o conhecimento transmitido ao longo do desenvolvimento deste trabalho.

A todos os colegas de trabalho que de alguma forma deixaram o dia a dia no laboratório mais leve e divertido. A todos do antigo grupo LEC e aos novos colegas do grupo Gent. Especialmente a Drª Fernanda Batista, Drª Marta Garcia, Drª Thayná Avelino, e Dr Helder Ribeiro, por sua amizade, por todo o conhecimento compartilhado, e principalmente por todas as rezas para o "desviramento de bucho" a cada experimento fracassado.

To my Frankfurter family - Lars, Cris, Elena, Pippo, Serena, Magnus, Lorenzo, and Judith - thank you for the daily laughs, waffles, and the privilege of experiencing German culture together. Above all, I would like to thank Dr. Sebastian Thallmair and Cristina Gil for their patience in explaining complex and abstract concepts to an experimentalist like me on several occasions. You've introduced me to the fascinating world of computational biology, and I've become genuinely captivated by it.

Aos meus pais pelo incentivo constante e por acreditarem em mim e no que eu poderia alcançar, mesmo que nem sempre compreendessem completamente o meu trabalho.

Ao meu companheiro, Matheus, com quem tenho o privilégio de dividir a vida, pelo suporte e paciência infinitos, pelas conversas e aprendizados diários. Sem você o caminho seria muito mais difícil.

Ao CNPEM e LNBio, pela infraestrutura e suporte técnico essenciais para a realização deste trabalho. À CAPES e à FAPESP, pelo apoio financeiro fundamental.

Este trabalho foi realizado com o apoio da Coordenação de Aperfeiçoamento de Pessoal de Nível Superior – Brasil (CAPES) – Código de Financiamento 001; e da Fundação de Amparo à Pesquisa do Estado de São Paulo (FAPESP), projetos: #2019/10274-7 e #2022/05028-0.

RESUMO

O receptor ativado por proliferador de peroxissoma gama (PPARγ) é um receptor nuclear responsável pela expressão de genes relacionados à adipogênese, a sensibilidade à insulina e a regulação metabólica geral. Recentemente, tem se destacado importância das modificações pós-traducionais, principalmente a fosforilação, na modulação da atividade do PPARγ. A fosforilação do PPARγ na serina 273 (S273) pela quinase dependente de ciclina 5 (CDK5) em condições de obesidade leva à desregulação de um subconjunto específico de genes-alvo do PPARγ envolvidos na sensibilidade à insulina. Por outro lado, a inibição da fosforilação S273 melhora a sensibilidade à insulina em modelos de obesidade em camundongos, apesar de alguns efeitos adversos, como o aumento da esteatose hepática. Este trabalho investiga os aspectos moleculares da fosforilação S273, demonstrando como essa modificação altera a conformação do PPARγ e consequentemente, sua afinidade por vários coreguladores. Nossos resultados revelam que a fosforilação em S273 diminui a interação do PPARγ com coativadores e aumenta sua associação com corepressores, modulando assim os padrões de expressão gênica essenciais para os processos metabólicos. A compreensão detalhada dos mecanismos moleculares envolvidos nessa fosforilação, estabelece um ponto de partida para o entendimento de efeitos e consequências mais abrangentes desse PTM na regulação metabólica. Nossas descobertas ressaltam a importância das modificações pós-traducionais na modulação da atividade do PPARγ e destacam o potencial de modular essas modificações para fins terapêuticos. A compreensão da regulação do PPARγ por meio da fosforilação da S273 é essencial para o desenvolvimento de novas estratégias de combate a doenças metabólicas.

ABSTRACT

Peroxisome proliferator-activated receptor gamma (PPARγ) is a nuclear receptor that regulates adipogenesis, insulin sensitivity, and overall metabolic regulation. Recent research highlights the significance of post-translational modifications, particularly phosphorylation, in modulating PPARγ activity. Phosphorylation of PPARγ at serine 273 (S273) by cyclin-dependent kinase 5 (CDK5) in obese conditions leads to dysregulation of a subset of PPARγ target genes involved in insulin sensitivity. Inhibiting S273 phosphorylation improves insulin sensitivity in mouse models of obesity despite some adverse effects like increased hepatic steatosis. This work investigates the mechanistic aspects of S273 phosphorylation, demonstrating how this modification alters PPARγ's conformation and its affinity for various coregulators. The study reveals that phosphorylation at S273 diminishes PPARγ's interaction with coactivators while enhancing its association with corepressors, thereby modulating gene expression patterns critical for metabolic processes. A detailed understanding of the molecular mechanisms involved in this phosphorylation provides a starting point for understanding the broader effects and consequences of this PTM on metabolic regulation. Our findings underscore the importance of post-translational modifications in modulating PPARγ activity and highlight the potential of targeting these modifications for therapeutic purposes. Understanding the regulation of PPARγ through S273 phosphorylation is essential for developing novel strategies against insulin resistance.

SUMÁRIO

1. INTRODUÇÃO

1.1. A obesidade é uma epidemia global

A prevalência global da obesidade tem atingido números alarmantes. Atualmente, quase um bilhão de pessoas, incluindo adultos e crianças, vivem com obesidade no mundo [1]. Nos últimos anos, o número de indivíduos obesos vem aumentando exponencialmente, com uma em cada oito pessoas convivendo com a obesidade em 20222 [2] . Essa tendência é particularmente acentuada em países subdesenvolvidos e em desenvolvimento, como o Brasil. Em 2019, 20,3% da população brasileira foi considerada obesa, com projeções indicando um aumento para aproximadamente 30% até 2030 [3] .

Atualmente a obesidade é considerada um problema de saúde pública, tendo impacto não só na mortalidade da população, como na incidência das comorbidades a ela associadas [4]. Com isso vê-se a necessidade da criação estratégias abrangentes para abordar as causas multifacetadas da obesidade. Sendo assim, torna-se imprescindível a compreensão dos mecanismos moleculares envolvidos nessa doença a fim de que possamos pensar em novas abordagens terapêuticas que possam prevenir ou tratar essa doença.

A obesidade é classificada como uma doença crônica debilitante, caracterizada pelo acúmulo excessivo de gordura, causado pelo desequilíbrio entre consumo e gasto energético [5] . Atualmente, o método utilizado para o diagnóstico leva em consideração o Índice de Massa Corporal (IMC), uma estimativa a partir das medidas de peso e a altura. Indivíduos com IMC maior do que 30 kg/m² são considerados obesos. Entretando, outros fatores como porcentagem de gordura corporal e lugares onde a gordura é distribuída também têm sido considerados nos diagnósticos modernos. A obesidade é uma doença complexa e influenciada por diversos fatores que interagem entre si. Agentes como a predisposição genética, padrões alimentares modernos e estilo de vida sedentário interagem entre si, contribuindo para sua ocorrência. Além disso, o contexto socioeconômico também desempenha um papel fundamental no surgimento e prevalência da doença [6].

O acúmulo excessivo de gordura corporal gera disfunções metabólicas em diversos órgãos, aumentando o risco das muitas comorbidades que são relacionadas à obesidade. Uma das consequências mais críticas da obesidade é o aumento do risco de diabetes tipo 2 (DT2) [7]. A obesidade é um dos principais fatores que contribuem para a resistência à insulina, levando a essa condição crônica que pode resultar em complicações graves, como insuficiência renal e amputações de membros. Além disso, as doenças cardiovasculares (CVDs), incluindo doenças cardíacas e derrames, também estão entre as principais causas de morte ligadas à obesidade [8]. O excesso de gordura corporal também pode levar à hipertensão, dislipidemia e outros fatores de risco para as CVDs. A obesidade também está ligada a vários tipos de cânceres, incluindo câncer de endométrio, de mama e de cólon, com estudos indicando que o risco aumenta proporcionalmente ao IMC [9]. Além desses problemas de saúde física, a obesidade também pode levar a problemas psicológicos, como depressão e ansiedade, complicando ainda mais o quadro de saúde dos indivíduos afetados.

Além da alta taxa de mortalidade, o custo que a obesidade representa para a sociedade é bastante elevado. O aumento da prevalência da obesidade representa desafios significativos para os sistemas de saúde. Portanto, a compreensão dos mecanismos moleculares da obesidade é essencial nesse contexto, pois permite o desenvolvimento de terapias direcionadas que abordam não apenas o controle de peso, mas também o tratamento e prevenção dessas comorbidades.

1.2. Características moleculares da obesidade

Uma das principais características da obesidade é a inflamação crônica sistêmica causada pelos altos níveis de ácidos graxos circulantes. Além dos adipócitos, células imunes também fazem parte do tecido adiposo, garantindo a integridade e sensibilidade hormonal, atuando em conjunto para regular o armazenamento e mobilização de energia em resposta às necessidades do organismo. Porém, em quadros de obesidade, as células do tecido adiposo operam em um estado pró-inflamatório. A grande quantidade de gordura saturada da dieta é detectada por sensores imunes, que acionam a síntese de citocinas inflamatórias e modificam o perfil da microbiota intestinal, que passa a

produzir metabólitos inflamatórios (LPS). Em conjunto, as citocinas pró-inflamatórias, ácidos graxos e lipossacarídeos bacterianos ativam uma rede de sinalização que gera alterações nas células metabólicas e imunes, como o deslocamento de macrófagos M1, ativação de células NK, produção de interferon y (INF-y) acúmulo de células CD8+ e polarização de linfócitos TH1 [10–12].

Uma das consequências da inflamação crônica associada à obesidade é o desenvolvimento de resistência à insulina, bem como aumento do risco de desenvolvimento de DT2 [7]. Os mecanismos que ligam a obesidade, inflamação e desregulação no mecanismo de sensibilidade à insulina tem atuação de citocinas pró-inflamatórias [10]. A abundância crônica de energia mantém a glicose plasmática a níveis constantemente elevados. Em resposta, há uma diminuição da resposta das células β às incretinas, como forma de reduzir o armazenamento excessivo de nutrientes, levando à resistência à insulina.

Diferentes vias metabólicas contribuem para o mecanismo de resistência à insulina, em especial IKK/NF-Kβ (quinase I kapa β /fator nuclear kapa β) e JNK1 (quinase N-terminal c-Jun 1) que têm papel-chave como link entre processos inflamatórios e metabólicos por meio da ativação de NF-kβ [13,14] . O mecanismo de resistência à insulina também é mediado pelo fator de necrose tumoral α (TNF-α), Interleucina 1 β (IL-1β) e proteínas quinases reguladas por sinal extracelular 1 e 2 (ERK1/2) [10,14]. Além de secretar elementos pró-inflamatórios derivados de macrófagos, os adipócitos hipertróficos ainda têm alta expressão e secreção de adipocinas pró-inflamatórias. Adicionalmente, os níveis plasmáticos de adiponectina, uma adipocina sensibilizadora da insulina, são reduzidos em indivíduos obesos [15].

1.3. O PPARγ é o regulador da adipogênese e metabolismo de glicose

Os processos citados anteriormente são decorrentes do acúmulo crônico de energia, que leva ao aumento em número (hiperplasia), e tamanho (hipertrofia) dos adipócitos, além da distribuição ectópica de gordura (dislipidemia) [2]. O principal responsável pelo processo de adipogênese é o Receptor Ativado por Proliferadores de Peroxissoma gama (PPARy). O PPARγ é o regulador dos genes envolvidos na diferenciação de células precursoras em adipócitos

maduros, que são essenciais para manter o equilíbrio energético e a homeostase metabólica [16] . A ativação do PPARγ aumenta a expressão de genes envolvidos na captação de glicose e no metabolismo de lipídios, melhorando assim a sensibilidade à insulina. No entanto, a desregulação da sinalização do PPARγ, muitas vezes exacerbada pela obesidade, leva à produção de citocinas pró-inflamatórias que contribuem para a resistência sistêmica à insulina.

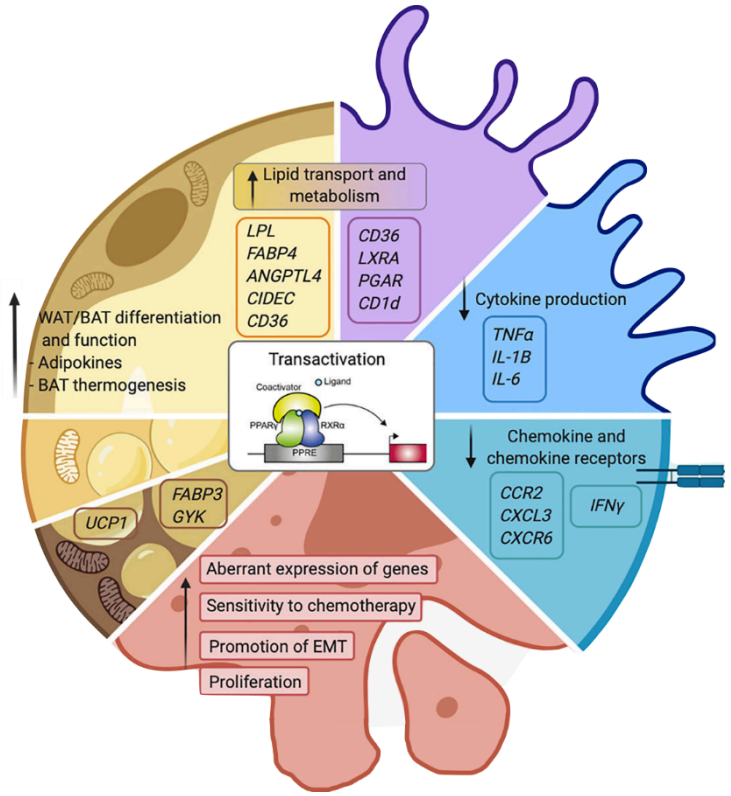

Figura 1. *Genes regulados por PPARγ nos diferentes tecidos*. Adaptado de: Hernandez-Quiles et al. Frontiers in Endocrinol (2021)

De modo geral, o PPARγ é o regulador mestre dos processos de diferenciação de adipócitos, metabolismo de glicose e sensibilidade à insulina (SI) em diferentes tecidos (Figura 1) [17]. Ele atua em células neuronais, onde tem papel neuro protetor, antioxidante e indutor da função mitocondrial [18]; também no intestino, onde tem papel anti-inflamatório e protetor da sensibilidade visceral; e no músculo esquelético, onde atua na oxidação de ácidos graxos e triglicerídeos, além de aumentar a captação de glicose. A ativação desse receptor também modula a expressão e secreção citocinas ligadas à imunidade, inflamação e

apetite [19] , como a leptina, molécula que atua na sinalização de fome e saciedade; a adiponectina, que está relacionada a sensibilidade à insulina, atuando no fígado e músculo esquelético; e a adipsina, associada a mecanismos anti-inflamatórios, e melhora da função de células β em casos de diabetes [20].

Estruturalmente, o PPARγ consiste em vários domínios funcionais (Figura 2) [21]. O domínio A/B N-terminal contém a função de ativação 1 (AF-1), que está envolvida na atividade transcricional independente de ligante e na ligação do coregulador. Em seguida, vem o domínio de ligação ao DNA (DBD), que apresenta dois motivos de dedo de zinco cruciais para o reconhecimento de sequências específicas de DNA conhecidas como elementos de resposta do proliferador de peroxissoma (PPREs). A região da “hinge” conecta o DBD ao domínio de ligação ao ligante (LBD), permitindo flexibilidade e facilitando as interações com o DNA e outras proteínas. O LBD é o maior domínio e contém a função de ativação 2 (AF-2), é onde ocorre interação com o ligante (LBP) e a dimerização do receptor com o receptor X retinóide (RXR) [21]. Essa estrutura modular permite que o PPARγ se envolva em várias interações intra e intermoleculares, influenciando sua capacidade de regular a expressão gênica em resposta a sinais metabólicos.

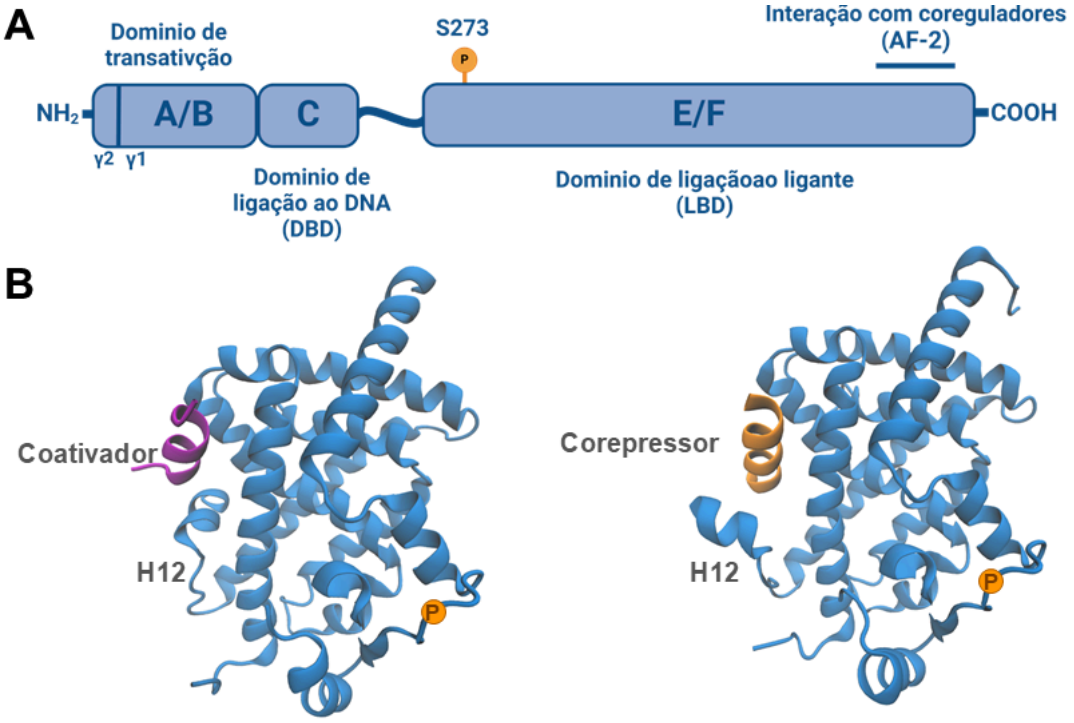

Figura 2. *Estrutura do PPARγ.* (A) Representação dos domínios do PPARγ. (B) Estrutura do domínio LBD do PPARγ destacando a H12, domínio importante para a interação com coativadores (peptídeo em roxo) e corepressores (em amarelo).

A atividade transcricional canônica do PPARγ ocorre por meio de sua interação com proteínas coreguladores, que podem ativar ou reprimir a transcrição gênica. Na ausência de ligantes, a conformação inativa da hélice 12 (H12) do domínio de ligação a ligantes (LBD) do PPARγ, favorece a ligação de proteínas corepressoras, que formam um complexo corepressor em conjunto com histonas desacetilases (HDAC) impedindo a transcrição do gene alvo [22]. Quando um ligante agonista ocupa o LBD, o receptor sofre uma alteração conformacional, que realoca H12, formando uma fenda carregada entre H3 e H4 [23]. Essa conformação leva à dissociação de corepressores e recrutamento de coativadores, formando um complexo coativador que recruta outras proteínas da maquinaria de transcrição, como as histonas acetiltransferases (HAT) e outros fatores gerais de transcrição, promovendo a transcrição do gene alvo.

Por causa de sua ação pleiotrópica o PPARγ é um alvo promissor nos estudos relacionados a desordens metabólicas. As tiazolidinedionas (TZDs) por exemplo, são uma classe de ligantes sintéticos que ativam o PPARγ, que foram amplamente como agentes antidiabéticos em pacientes com DT2 [24]. Ao promover a diferenciação de adipócitos e aumentar a captação de glicose nos tecidos periféricos, a ativação do PPARγ ajuda a reduzir os níveis de açúcar no sangue e a atenuar a resistência à insulina. Entretanto, as TZDs foram associadas a efeitos colaterais indesejáveis, como ganho de peso e aumento do risco de problemas cardiovasculares, o que limitou seu uso [25] .

Atualmente, sabe-se que os efeitos colaterais observados no tratamento com as TZDs são consequência da forte ativação que do PPARγ. Apesar disso, sua atuação como sensor lipídico e modulador de diversas respostas metabólicas faz do PPARγ um alvo amplamente estudado quando se trata de desenvolvimento de fármacos para o tratamento de obesidade e DT2. Os avanços recentes nos estudos de medicamentos antidiabéticos direcionados ao PPARγ se concentraram em melhorar a eficácia e, ao mesmo tempo, minimizar os efeitos colaterais associados aos agonistas clássicos [26].

Novas estratégias de modulação do PPARγ incluem novos ligantes derivados dos TZDs, que o ativem, mas não produzam os efeitos colaterais; Desacetilação do receptor - estudos indicam que a desacetilação do PPARγ pode melhorar o índice terapêutico dos TZDs [27]; Ligantes não agonistas e moduladores seletivos de PPARγ (SPPARMs) - classe de medicamentos desenvolvidos para proporcionar uma modulação mais sutil da atividade do PPARγ [28]; Modulação de Modificações pós-traducionais (PTMs), que ocorrem em consequencia da desregulação metabólica [29,30] .

Os diversos estudos que tem o PPARγ como um alvo terapêutico refletem sua função crítica na regulação da saúde metabólica. Este trabalho busca aprofundar o conhecimento sobre a modulação das modificações pós-traducionais (PTMs) do PPARγ, com foco especial na fosforilação do resíduo S273, como uma estratégia para tratar a resistência à insulina.

1.4. Uma fosforilação do PPARγ está diretamente ligada a obesidade

As modificações pós-traducionais (PTMs) são mecanismos regulatórios essenciais que influenciam a função, a estabilidade e as interações das proteínas, principalmente no contexto da obesidade. Entre essas modificações, a fosforilação desempenha um papel fundamental na modulação da atividade das principais proteínas envolvidas nos processos metabólicos. Na obesidade, a desregulação dos eventos de fosforilação pode afetar significativamente as vias de sinalização da insulina, levando à resistência à insulina [31]. Por exemplo, a fosforilação de resíduos específicos em proteínas como o PPARγ pode alterar sua atividade e interações com outras moléculas de sinalização, afetando, em última análise, a absorção de glicose e o metabolismo lipídico. Esse mecanismo faz parte do ajuste fino da atividade do PPARγ e pode alterar a tanto a estabilidade do receptor, quanto sua atividade, alterando a interação do receptor com outras proteínas regulatórias, como os coreguladores.

Em específico, uma fosforilação no resíduo 273 no domínio de interação com ligantes (LBD) do PPARγ, tem sido associada com o contexto de obesidade e RI. Essa modificação é mediada pela quinase dependente de ciclina (CDK5), enzima ativada por estímulos pró-inflamatórios e ácidos graxos circulantes, que são elevados em quadros de obesidade.

O estado inflamatório característico de quadros de obesidade, induz a níveis elevados de TNF-α, IL-6 e outras citocinas pró-inflamatórias que são secretadas pelo próprio tecido adiposo. Essas citocinas ativam a CDK5 promovendo a clivagem de seu ativador, p35, gerando sua forma ativa, conhecida como p25 [32]. A p25 em sua forma ativa aumenta a atividade de quinase da CDK5, levando à fosforilação dos principais substratos, incluindo o PPARγ na serina 273 (S273) [33].

A fosforilação da S273 afeta a expressão de adipocinas sensibilizadoras de insulina, como a adiponectina, uma adipocina que desempenha um papel fundamental no aumento da sensibilidade à insulina e na regulação dos níveis de glicose. Além disso, também diminui a expressão da adipsina, outra adipocina envolvida no sistema complementar e na regulação metabólica [33]. Essa desregulação contribui para um estado pró-inflamatório caracterizado pelo aumento da expressão de citocinas inflamatórias, intensificando ainda mais a disfunção metabólica. Entretanto, foi demonstrado que essa modificação não altera a capacidade adipogênica do receptor, nem sua ocupância no DNA [33–35].

Um trabalho recente demonstrou que quando o PPARγ é fosforilado na S273, ele promove a expressão do fator de diferenciação do crescimento 3 (GDF3), que demonstrou inibir as vias de sinalização da insulina [36]. Através de modelos de camundongos geneticamente modificados para impedir a fosforilação da S273, foi demonstrado que a ausência da fosforilação induz a uma melhora na sensibilidade à insulina, sem alterações no peso corporal indicando que o evento de fosforilação em si é um fator fundamental no desenvolvimento da resistência à insulina.

Atualmente, diversos ligantes de PPARγ, incluindo as TZDs, são capazes de impedir que essa fosforilação aconteça, o que leva uma melhora na sensibilização à insulina [37–39]. Tais ligantes não fazem contato direto com o resíduo 273, mas induzem modificações estruturais na interface de interação PPARγ-CDK5, protegendo o sítio de ser fosforilado [33,40]. Essa proteção ocorre por meio da estabilização de regiões flexíveis o PPARy, como a porção final da alça H2-H2′ e, principalmente, a hélice H2′, em conformação desfavorável para o acoplamento da CDK5 [40].

A descoberta da fosforilação do resíduo S273 no PPARγ marcou uma mudança nas estratégias de modulação do PPARγ e impulsionou o desenvolvimento de ligantes não agonistas capazes de inibir essa modificação

específica. Esses compostos podem dissociar as propriedades de sensibilização à insulina dos efeitos colaterais de transcrição normalmente associados aos agonistas completos. Sendo assim, a compreensão detalhada de como as modificações pós-traducionais (PTMs) afetam a função do PPARγ é essencial para abrir novos caminhos no design de fármacos.

1.5. Entendendo o mecanismo de ação do PPARγS273$_{po4}$

O entendimento dos mecanismos e das consequências da fosforilação S273 do PPARγ é essencial para o desenvolvimento de novos alvos terapêuticos para distúrbios metabólicos. No geral, é sabido que a fosforilação das proteínas pode contribuir para o aumento da atividade coativadora, ao mesmo tempo que diminui atividade dos corepressores 34. Entretanto, a fosforilação da S273 parece promover atividade corepressora de proteínas associadas ao PPARγ.

Foi demonstrado que o corepressor THRAP3 (proteína associada ao receptor do hormônio tireoidiano 3), interage diretamente com o receptor especificamente quando a S273 está fosforilada [41], alterando a expressão de alguns genes controlados pelo PPARγ, e induzindo uma redução na sensibilidade à insulina. Além disso, o corepressor nuclear 1 (NCoR) também foi associado a esse PTM. Nesse caso, O NCoR atua como uma proteína adaptadora que aumenta a capacidade do CDK5 de se associar e fosforilar o PPARγ, promovendo assim um estado de resistência à insulina [42]. Esses achados levantaram novos questionamentos sobre o mecanismo de interação entre essas proteínas e como isso se relaciona a resposta metabólica diferencial frente a presença ou ausência desse PTM.

Um artigo anterior do grupo caracterizou mutantes de PPARγ, com foco específico na fosforilação do resíduo S273 (equivalente ao S245 na isoforma 1 de PPARγ). Esse trabalho demonstrou que a mutação não interfere na estrutura da proteína, preservando sua integridade estrutural e, consequentemente, viabilizando a análise funcional. Além disso, a pesquisa elucidou a interface de interação entre PPARγ e CDK5, identificando os resíduos âncora que são essenciais para essa interação. Em um estudo subsequente, o mesmo grupo utilizou camundongos knockin com mutantes S273A, evidenciando que a inibição

completa da fosforilação de S273 resulta em efeitos adversos no organismo, impactando diversos marcadores metabólicos, especialmente no fígado. Com base nessas evidências, o presente trabalho visa avançar na compreensão dos mecanismos subjacentes à fosforilação de S273, proporcionando uma análise mais detalhada dos efeitos dessa modificação pós-traducional na fisiologia metabólica.

Neste trabalho nós exploramos os mecanismos pelos quais a fosforilação da S273 induz a expressão diferencial dos genes relacionados a resistência à insulina. Nossa hipótese inicial é de que a desregulação genica causada pela fosforilação ocorre devido a alteração nas interações entre o PPARγ fosforilado e várias proteínas coreguladores, o que pode alterar o equilíbrio entre a ativação e a repressão de genes nos adipócitos.

No primeiro artigo, investigamos a influência da fosforilação na interação entre PPARγ e seus coreguladores. Focamos em cinco coreguladores específicos e descobrimos que a fosforilação da S273 reduz a interação com coativadores como PGC1-α, TRAP220 e TIF2, ao mesmo tempo que aumenta a ligação com corepressores como NCoR e SMRT. Além disso, analisamos a interação com a CDK5 e seu impacto sobre esses coreguladores. Nossos resultados elucidam não apenas as consequências da fosforilação do PPARγ, mas também o próprio processo de fosforilação, destacando o papel contínuo da CDK5 quando acoplada ao receptor.

No segundo artigo, aprofundamos a investigação sobre como a fosforilação da altera a estrutura e a dinâmica do PPARγ. Utilizando simulações computacionais, identificamos as regiões afetadas pela fosforilação e os possíveis impactos dessas alterações. Nossos resultados mostram que a fosforilação não apenas afeta a dinâmica dos resíduos próximos à S273, mas também influencia regiões estruturalmente distantes. Observamos que a fosforilação atua de forma alostérica, modulando a interação diferencial com os coreguladores, conforme descrito no primeiro artigo.

Essas descobertas fornecem novas percepções sobre os mecanismos de regulação da expressão gênica e podem ajudar a pavimentar novos caminhos para modulação do PPARγ de forma eficaz e alternativa ao agonismo clássico.

2. DOCUMENTO PUBLICADO

2.1. Artigo I - PPARγ S273 phosphorylation modifies the dynamics of coregulator protein recruitment

Open Access Published: 26 November 2020 doi: https://doi.org/10.3389/fendo.2020.561256

Author names and affiliations:

Marieli Mariano Gonçalves Dias[1,2] Fernanda Aparecida Heleno Batista[1] Thais Helena Tittanegro[1] André Gustavo de Oliveira [3,4] Albane Le Maire,Albane Le Maire [1,5] Felipe Rafael Torres1 Helder Veras Ribeiro Filho[1] Leonardo Reis Silveira [3,4] Ana Carolina Migliorini Figueira[1,2*]

[1]Brazilian Biosciences National Laboratory (LNBio), Brazilian Center for Research in Energy and Materials (CNPEM), Campinas, Brazil

[2]Graduate Program in Functional and Molecular Biology, Institute of Biology, State University of Campinas (Unicamp), Campinas, Brazil

[3]Mitochondrial Molecular Biology Laboratory, Obesity and Comorbidities Research Center (OCRC), Campinas, Brazil

[4]Department of Structural and Functional Biology, Institute of Biology, University of Campinas (UNICAMP), Campinas, Brazil

[5]Centre de Biochimie Structurale CNRS, Université de Montpellier, Montpellier, France

Keywords: PPAR gamma, Coregulator interaction, Coactivator, Corepressor, Ser273 phosphorylation

ABSTRACT

The nuclear receptor PPARγ is essential to maintain whole-body glucose homeostasis and insulin sensitivity, acting as a master regulator of adipogenesis, lipid and glucose metabolism. Its activation through natural or synthetic ligands induces to the recruitment of coactivators, leading to transcription of target genes such as cytokines and hormones. More recently, post-translational modifications, such as PPARγ phosphorylation at Ser273 by CDK5 in adipose tissue, have been linked to insulin resistance through the deregulation of expression of a specific subset of genes. Here, we investigate how this phosphorylation may disturb the interaction between PPARγ and some coregulator proteins as a new mechanism that may leads to insulin resistance. Through cellular assays, we show that PPARγ phosphorylation

increased the activation of the receptor, therefore the increased recruitment of PGC1-a and TIF2 coactivators, whilst decreases the interaction with SMRT and NCoR corepressors. Moreover, our results show a shift in the coregulator's interaction domain preferences, suggesting additional interaction interfaces formed between the phosphorylated PPARγ and some coregulator proteins. Also, we observed that the CDK5 presence disturbs the PPARγ-coregulator's synergy, decreasing interaction with PGC1-a, TIF2, and NCoR but increasing the coupling of SMRT. Finally, we conclude that the insulin resistance provoked by PPARγ phosphorylation is linked to a disbalance in coregulator proteins, which may promote the dysregulation in gene expression.

INTRODUCTION

Peroxisome proliferator-activated receptor gamma (PPARγ) is closely linked to energy homeostasis regulation because it plays important roles in adipogenesis, lipid and carbohydrate metabolism, insulin sensitivity, cell proliferation, and inflammatory processes. This nuclear receptor (NR) acts as a metabolic sensor of dietary lipids and is considered of extreme importance as a metabolism modulator [1,2], regulating diabetes through cytokines and hormones, such as TNFα and leptin [2–4], secretion. Like other NR superfamily members, PPARγ is activated by natural ligands, like some fatty acids and their metabolites, and by synthetic ligands such as Rosiglitazone and Pioglitazone (Thiazolidinediones - TZDs), which are insulin sensitizers used in type 2 diabetes treatment.

The canonical transcriptional activity of PPARγ occurs through its interaction with several cofactors, which activate or suppress gene transcription. In the absence of ligands, the inactive conformation of helix 12 (H12) of the PPARγ ligand binding domain (LBD) favors the binding of corepressor proteins, such as silencing mediator of retinoid and thyroid hormone receptor (SMRT) and the nuclear receptor corepressor 1 (NCoR). These proteins form a corepressor complex with histone deacetylases (HDAC) repressing target gene transcription [5]. In the presence of ligands, the receptor undergoes a conformational change that reallocates H12, forming a charge clamp between H3 and H12[6]. This conformation leads to corepressors dissociation and coactivator recruitment, forming a coactivator complex

by the recruitment of other proteins, as well as histone acetyltransferases (HAT) and other general transcription factors, promoting the transcription of the target gene [7].

Beyond this canonical transcriptional activity, PPARγ can also be regulated by post-translational modifications (PTMs), such as acetylation, phosphorylation, SUMOylation, and ubiquitination [8].These fine-tuning adjust is part of the cell or tissue-specific modulation [9,10] and can dramatically alter the receptor function, as well as its binding to coregulators [11]. By all these PTMs, the PPARγ phosphorylation is one of the most studied and may promote different receptor behavior, depending on the residue in which it occurs and on the enzyme that performs the phosphorylation and/or dephosphorylation [12,13].

Most of PPARγ phosphorylations were described on its N-terminal domain. The phosphorylation of Y78 is regulated by SRC proto-oncogene, nonreceptor tyrosine kinase (c-SRC), and Protein-tyrosine phosphatase 1B (PTP-1B) and affects the inflammatory response and insulin sensitivity [14]. The phosphorylation in S112 by Mitogen-Activated Protein Kinases (MAPKs) pathway [15,16] , and by the Cyclin-Dependent Kinases 7 (CDK7) and 9 (CDK9) [17,18] intensifies the interaction between PPARγ and the circadian clock protein PER2 (Period Circadian Regulator 2) [19], decreasing PPARγ activation through the reduction of both coactivator binding [15] and ligand binding affinity [20]. In addition, S133 and T296 residues were also identified as targets for Extracellular Signal-Regulated Kinase (ERK)/ Cyclin-Dependent Kinase 5 (CDK5) phosphorylation pathway [21].

Particularly, one special obesity-mediated phosphorylation targeting PPARγ ligand binding domain (LBD), reported in the last decade, has been associated with insulin resistance [22,23]. This phosphorylation, performed by the CDK5 at PPARγ S273 (or S245 in isoform 1), does not alter the adipogenic activity of PPARγ but deregulates a subset of genes that presented altered expression in obesity and diabetes, as adiponectin and adipsin [22,23]. It is known that this phosphorylation does not change the occupancy of PPARγ in the chromatin [23]The mechanism that correlates this phosphorylation to deregulate these specific genes is still unknown.

Various PPARγ ligands can inhibit this phosphorylation. One of them is the TZDs insulin-sensitizer class of drugs, which owns familiar anti-diabetic actions but presents negative side effects due to its strong agonism. On the other hand, some

partial agonists, such as MRL24 [22], SR1664 [23], GQ-16 [24], UHC1 [25], F12016 [26], L312 [27], Chelerythrine [28], and AM-879 [29], have been identified to inhibit this PTM without the agonist activity. Structural data analysis showed that PPARγ ligands that inhibit S273 phosphorylation do not directly contact this residue but induce structural modifications in the PPARγ:CDK5 interaction interface. Such ligands fit into binding pockets, promoting an interaction network that protects S273, blocking its phosphorylation [30]Therefore, the most recent strategy of PPARγ modulation targets the partial agonism of receptors, aiming at phosphorylation inhibition.

Mastery and manipulation of the mechanisms involved in this phosphorylation pathway can be a promising approach to improving metabolic disorders therapies. It is known that phosphorylation on some coregulators may contribute to increased coactivator and decreased corepressor activity [31]. One recent study reported that the Thyroid Hormone Receptor 3-Associated Protein (THRAP3), directly interacts with PPARγ specifically when S273 is phosphorylated, acting as a specialized coregulator that docks on certain phosphorylated transcription factors [32]. Moreover, the corepressor NCoR was reported as an adaptor protein that enhances the ability of CDK5 to associate with and phosphorylate PPARγ [33].

Here, we demonstrate that the dysregulation caused by Ser273 phosphorylation might occur through the differential recruitment of coregulatory proteins, causing differences in the target gene expression. By using five coregulators reported to interact with PPARγ in adipogenesis, the coactivators PGC1-α, TRAP220, and TIF2, and the SMRT and NCoR corepressors [34–37] we evaluated that the PPARγ S273 phosphorylation modifies its interaction with coregulators. Our results show that the presence and absence of phosphorylation at S273 can alter PPARγ activation and its interaction profile with some coregulators. The absence of phosphorylation can lead to an increased activation of PPARγ due to a higher interaction with coactivators and decreased interaction with corepressors. Additionally, the CDK5 presence also disrupts this coregulator harmony. Finally, we hypothesize that additional interfaces may be formed in coregulators – PPARγ interaction.

METHODS

Plasmids

pBIND-PPARγ harboring a chimeric protein composed of Gal4 DBD and the PPARγ LBD region (aa 238-503), pGRE-LUC (containing the upstream activating sequence of Gal4 followed by a firefly luciferase reporter gene), pRL-TL (which constitutively express *Renilla reniformis* luciferase, used as transfection control for vector normalization). All the coregulators constructs were inserted into the commercial vector pM (Clontech), which contains the Gal DBD. The Gal- PGC1-a (containing mouse PGC1-a from 136 to 340 amino acids) and Gal-TRAP220 (ID1 + ID2 containing human TRAP220 from 404 to 654 amino acids) are plasmids belonging to the Laboratory of Spectroscopy and Calorimetry *(LEC,* LNBio / CNPEM*, Brazil)*. Gal–TIF-2 (harboring three interaction domains of human TIF-2 from 624 to 869 amino acids), Gal–SMRT (ID1 + ID2, containing human SMRT from 982 to the C terminus), Gal–NCoR (ID1 + ID2 + ID3 containing mouse NCoR from 1629 to the C terminus), and VP16-PPARγ (harboring the chimeric protein of the LBD region of PPARγ with the transactivation domain of the VP16 Human herpes simplex virus 2) were kindly provided by Dra. Albane Le Maire from Centre de Biochimie Structurale *(CBS, CNRS, France).* The plasmid pCDNA3-Cdk5 (which encodes the Cdk5 and P35 proteins) were kindly provided by Professor Sang K. Park of *Pohang University of Science and Technology.*

Mutations

To evaluate whether S273 phosphorylation would alter both the activation of PPARγ and its interaction with coregulators, we mutated this residue (target of phosphorylation) in order to mimic the phosphorylated serine and the inhibition of phosphorylation. Mutations of pBIND-PPARγ and VP16-PPARγ at S273 to alanine (PPARγ S273A), used as a constitutive dephosphorylation PPAR form, and to aspartic acid (PPARγ S273D), used to mimic phosphorylation [38] were performed using Quick Solution of QuickChange site-directed mutagenesis kit (Promega) with pFU DNA polymerase (Promega).

This same strategy generated Gal-PGC1-α, Gal-TIF2, Gal–SMRT, and Gal-NCoR derivatives harboring mutated interaction domains. To inactivate each ID, for alanines substituted coactivators two specific leucines, as Gal-PGC1-α domain LKKLL was mutated to LKKAA (residues 142-146, Gal4-PGC1-α ID1m), Gal-TIF2 had the ID1(residues 641-645) changed from LLQLL to LLQAA (Gal-TIF2 ID1m), the ID2 (residues 689 – 694) changed from LHRLL to LHLAA (Gal-TIF2 ID2m), and the ID3 (residues 744 – 749) changed from LRYLL to LRYAA (Gal-TIF2 ID3m). For corepressors, the specifics isoleucine were replaced by alanine, as Gal-SMRT had the ID1 (residues 2094-2098) changed from ISEVI to ISEAA (Gal-SMRT ID1m), and the ID2 (residues 2296-2300) changed from LEAII to LEAAA (Gal-SMRT ID2m), and Gal-NCoR had the ID1 (residues 2073-2077) changed from ICQII to ICQAA (Gal-NCoR ID1m), the ID2 (residues 2277-2281) changed from LEDII to LEDAA (Gal-SMRT ID2m), and the ID3 (residues 1932-1937) changed from IDVII to IDVAA (Gal-SMRT ID3m). The used primers are listed in the supplementary material and all the mutations and constructs were verified by DNA sequencing.

Cellular assays

COS-7 and 293T cells were cultured in DMEM (Dulbecco's Modified Eagle's Medium) supplemented with 10% Bovine Fetal Serum (FBS), 1% antibiotics (penicillin and streptomycin), and 0.37% sodium bicarbonate and kept in a humid incubator, at 37 ° C and 5% CO_2. Plasmids transfections were performed using 400ng of each plasmid and the JetPEI (Polyplus) transfecting agent in a 3:1 ratio. 24 hours after transfection, 1uM of Rosiglitazone was added to the plate, which was incubated for 24 hours. The cells were lysed and assayed for reporter expression. Luciferase was measured using the Dual-Luciferase® Reporter Assay System kit (Promega). Luminescence reading was performed on the GloMax®-Multi Detection System reader. In each case, we normalized results by co-expressed *Renilla luciferase* signal. We carried out each transfection in triplicate and repeated each assay three to eight times [39].

To measure possible changes in PPARγ activation in different phosphorylation states, transactivation assays were performed on Hek293T cells with transient transfection of plasmids pBIND-PPARγ, pBIND-PPARγ S273A, pBIND-PPARγ

S273D, pGRE-LUC, pRL-TL as transfection control, and pCDNA3-CDK5. To measure the interaction between coregulators and PPARγ and possible differences due to different receptor phosphorylation states, mammalian two-hybrid assays were performed in Hek293T cells for corepressor assays and COS-7 for coactivators assays. The plasmids used were VP16-PPARγ, VP16-PPARγ S273A, VP16-PPARγ S273D, Gal-Coregulators (PGC1-α, Gal-TRAP220, Gal-TIF2, Gal-SMRT, Gal-NCoR, and its mutated derivatives), pGRE-LUC, pRL-TL as transfection control, and pCDNA3-CDK5.

The luminescence value was corrected by transfection control (luciferase Firefly/Renilla), and the value of each tested condition was divided by the luminescence value of the experimental control to obtain the activation rate. As negative control of transactivation assays, an empty pCDNA3.1 vector was used. For mammalian two-hybrid assays, the luminescence value of each tested condition was divided by the baseline condition of the experiment, which for the corepressors is the corepressor tested without the presence of PPARγ, and for the coactivators, it is the empty Gal4 vector to obtain the interaction rate [40–42]. Data analysis was performed with GraphPad Prism by two-way ANOVA, comparing the groups treated with Rosiglitazone and untreated of each PPARγ by Bonferroni's test, with values of p <0.05 / ** 0.001 / * ** 0.001.

Protein expression and purification

PPARγ (207-477) expression and purification were performed as previously described [29]. NCoR (2059-2297) expression was performed in the Escherichia coli BL21 (DE3) strain. Cells were grown in Luria-Bertani medium (LB), at 37 °C, until OD_{600nm} = 0.8 and were induced with 1mM Isopropyl β-d-1-thiogalactopyranoside (IPTG) and 10uM $ZnCl_2$, at 22 °C for 16h, 200RPM. Then, bacteria were harvested by centrifugation (20 min at 16,000 RCF at 4°C), and the pellet was resuspended in lysis buffer (20mM Tris–HCl pH 7.5, 300mM NaCl, 5% glycerol, 2mM β-mercaptoethanol, 100mM PMSF and 1 mg lysozyme). After 1 h at 4 °C, the extract was sonicated on an ice bath, and the soluble fraction was separated by centrifugation at 36,000 RCF for 1h at 4°C. Purification was performed on an FPLC-GE Healthcare (4°C) HiTrap Chelating 5mL HP-GE Healthcare column. The

entire equilibration, sample injection, washing, and elution process was performed at 1mL / min. Column equilibration was done with 2% buffer B (20mM Tris–HCl pH 7.5, 300mM NaCl, 5% glycerol, 2mM β-mercaptoethanol, 100mM PMSF, and 500mM Imidazole); sample injection was done in buffer A (20mM Tris–HCl pH 7.5, 300mM NaCl, 5% glycerol, 2mM β-mercaptoethanol, 100mM PMSF and 1 mg lysozyme); and elution was done on a linear gradient of 30 volumes of Buffer B column until it reached 100%.

SMRT (2041-2359) was co-expressed with PPARγ LBD. The expression was performed in a modified Escherichia coli BL21(DE3) strain (de Marco, A. et al., 2007). Cells were grown in LB medium, at 37 °C until OD_{600nm} = 0.88 and were induced with 1mM Isopropyl β-d-1-thiogalactopyranoside (IPTG) at 18°C for 16h, 200RPM. Then, bacteria were harvested by centrifugation (20 min at 16,000 RCF at 4°C), and the pellet was resuspended in lysis buffer (10mM NaH_2PO_4 pH 7.4, 140mM NaCl, 2.7mM KCl, 1mM β-mercaptoethanol). After 1 h at 4°C, the extract was sonicated on an ice bath, and the soluble fraction was separated by centrifugation at 36,000 RCF for 1h at 4 °C. Purification was performed in two steps. First, the supernatant was incubated with previously equilibrated Talon cobalt resin (Clontech) with equilibration buffer (PBS pH7.4, 10mM NaH_2PO_4 pH 7.4, 140mM NaCl, 2,7mM KCl) for 1h. After 1h, the resin solution was transferred to a plastic column, and flow through was collected. The resin was washed with (5mM Imidazole, 1mM β-mercaptoethanol, PBS pH7.4) and fractions were eluted with 5mL of elution buffer (PBS pH 7.4, 10mM NaH_2PO_4 pH 7.4, 140mM NaCl, 2,7mM KCl, 300mM Imidazole). The entire purification process was performed at 4° C. In the second step, the eluted fractions were incubated in previously equilibrated Glutathione Sepharose 4B GST-tagged resin (GR Healthcare) for 3h. After that, the resin solution was transferred to a plastic column, and flow through was collected. The resin was washed with (10mM NaH_2PO_4 pH 7.4, 140mM NaCl, 2,7mM KCl, and 1mM β-mercaptoethanol), and fractions were eluted with elution buffer (60mM Tris pH 8.0, 10mM reduced glutathione, 1mM β-mercaptoethanol).

In vitro phosphorylation assay

CDK5-mediated phosphorylation of PPARγ and the complexes with SMRT and NCoR corepressors was measured by luminescent detection of ADP produced in the in vitro phosphorylation reaction, as it was described in [29]. We used ADP-Glo™ kinase assay (Promega) following manufacturer's instructions, in which 15 μM of purified PPARγ LBD and the complexes PPARγ+SMRT and PPARγ+NCoR were incubated with 25 ng of purified CDK5/p35, at room temperature for 15 min, in the kinase assay reaction buffer (200mM Tris-HCl, pH 7.4, 100mM MgCl2 and 0.5 mg/ml BSA, SignalChem kinase assay buffer III) in the presence of ATP 10 μM, in 12,5 μL of reaction volume. After the kinase reaction, ADP-Glo™ Reagent was added, and the reaction was incubated at room temperature for 40min. Then, the samples were denaturated at 95 °C for 30. After this step, the Kinase Detection Reagent was added, and the samples were incubated at room temperature for 30min. The luminescence signal was recorded using GloMax-Multi+Detection System (Promega) microplate luminometer. Statistical analysis was performed with GraphPad Prism, by t-test, with values of p < * 0.05 / ** 0.001 / *** 0.001.

RESULTS

The absence of phosphorylation increases PPARγ activation.

To measure possible differences in the PPARγ activation due to S273 phosphorylation, we performed a gene reporter assay comparing the activation of PPARγ wild-type (wt), PPARγ S273A, a phosphorylation-defective mutant, and PPARγ S273D, a structural phosphomimetic mutant. Additionally, we measured the PPARγ wt activation in the presence of CDK5, the enzyme responsible for PPARγ S273 phosphorylation. The Rosiglitazone induced PPARγ activation in a similar way for both wt and phosphorylated conditions (PPARγ wt, PPARγ S273D, and PPARγ + CDK5), presenting a rate of fold activation of 115, 110, and 100, respectively (Figure 1). These results imply that the phosphomimetic mutant behaves close to PPARγ wt in the presence and the absence of CDK5 (PPARγ + CDK5), validating the use of this mutant to mimic PPARγ phosphorylation situations. Moreover, these results suggest that PPARγ wt possibly is phosphorylated in our cellular assay conditions.

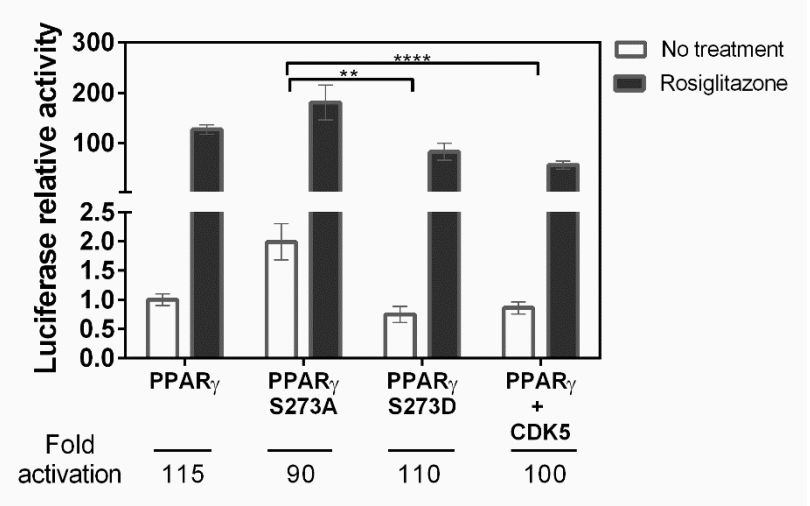

Figure 1 – *Activation of PPARγ in different phosphorylation states*. Transactivation assay with reporter gene in mammalian cells (Hek293T) was used to evaluate the activation profile of PPARγ wt and its mutants in the presence and absence of the Rosiglitazone. The PPARγ S273A mutant prevents the occurrence of phosphorylation, the PPARγ S273D mutant is a structural phosphomimetic. The CDK5 enzyme is responsible for the phosphorylation of PPARγ in S273. It is possible to observe that phosphorylation prevention increases the activation of PPARγ. Eight assays were performed in biological triplicate with n = 24. Statistical analysis: one-way ANOVA. p-value: p <0.05 *; p <0.001 *; p <0.001 ***. The phosphorylation inhibitor mutant had greater activation relative to the other conditions

On the other hand, the PPARγ S273A mutant presented the highest absolute value of Rosiglitazone-induced activation among all the mutants. However, its activation fold was the lowest (90-fold). This lower activation ratio is a reflex of the increased basal activation of this mutant (no treatment) that doubled compared to PPARγ wt basal activation. These results suggest that the inhibition of S273 PPARγ phosphorylation increases this receptor's activation, which may be associated with an enhanced dissociation of corepressors and/or an improvement in coactivator recruitment.

The absence of S273 phosphorylation increases both the coactivator's coupling and the corepressor's dissociation.

To evaluate if phosphorylation could be able to increase coactivator and/or decrease corepressor interaction with PPARγ, we perform mammalian two-hybrid assays comparing PPARγ interaction with the selected coregulators (PGC-1, TRAP220, TIF2, NCoR, and SMRT). Firstly, we measured the PPARγ binding preferences with the chosen coregulators (Figure 2). The results show that within the coactivators, PGC1-α had the highest interaction with PPARγ (7-fold), followed by

TRAP220 (4-fold). Interestingly, our construct of TIF2 did not present significant changes in its interaction due to ligand responsiveness, suggesting low PPARγ binding due to the agonist effect. Among the corepressors, both showed a similar dissociation rate, in the presence of the ligand, of 65% and 64%, respectively, for SMRT and NCoR. In addition, the initial interaction rate (No treatment) of SMRT is higher, suggesting a preferential binding to PPARγ.

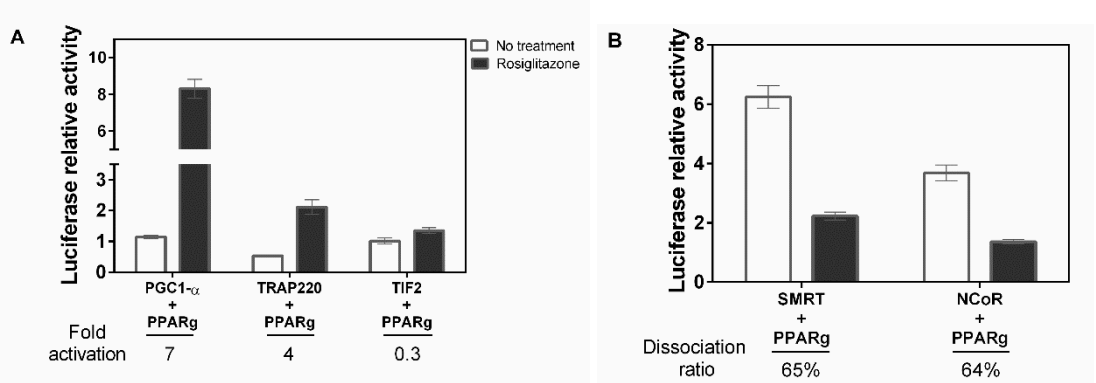

Figure 2– *Affinity of different coregulators with PPARγ.* A) The interaction with the PGC1-alpha coactivator was the highest among the coactivators studied, followed by TRAP220, which maintains the high activation due to the ligand. The TIF2 coactivator did not have a large increase in the presence of the ligand. (n=15) B) Among the compressors, the SMRT had higher affinity than NCoR (n=9). Statistical analysis: one-way ANOVA. p-value: p <0.05 *; p <0.001 *; p <0.001 ***.

Furthermore, we measured the coregulator's interaction with PPARγ in different phosphorylation states by using a mammalian two-hybrid assay. Despite having different interaction rates, TIF2 and PGC1-a coactivators (Figures 3A and 3C) presented similar interaction profiles with the PPARγ wt, PPARγ S273A and PPARγ S273D, both presenting higher interaction with phosphorylation-defective mutant (S273A). Yet, the interaction with the phosphomimetic mutant (S273D) presented similar behavior to the wt receptor, indicating that these coactivators binding are sensitive to S273 phosphorylation and suggesting an increased binding of these coactivators in the absence of PPARγ phosphorylation. This interaction profile agrees with the activation profile seen in Figure 1, confirming that the lack of phosphorylation might increase coactivators binding. Nevertheless, the TRAP220 did not show interaction changes with the receptor in any phosphorylation state, suggesting that its binding to the receptor depends solely on the classical interaction surface formed by the receptor's H12 closing where the LXXLL motif of the coactivator binds (Figure 3B).

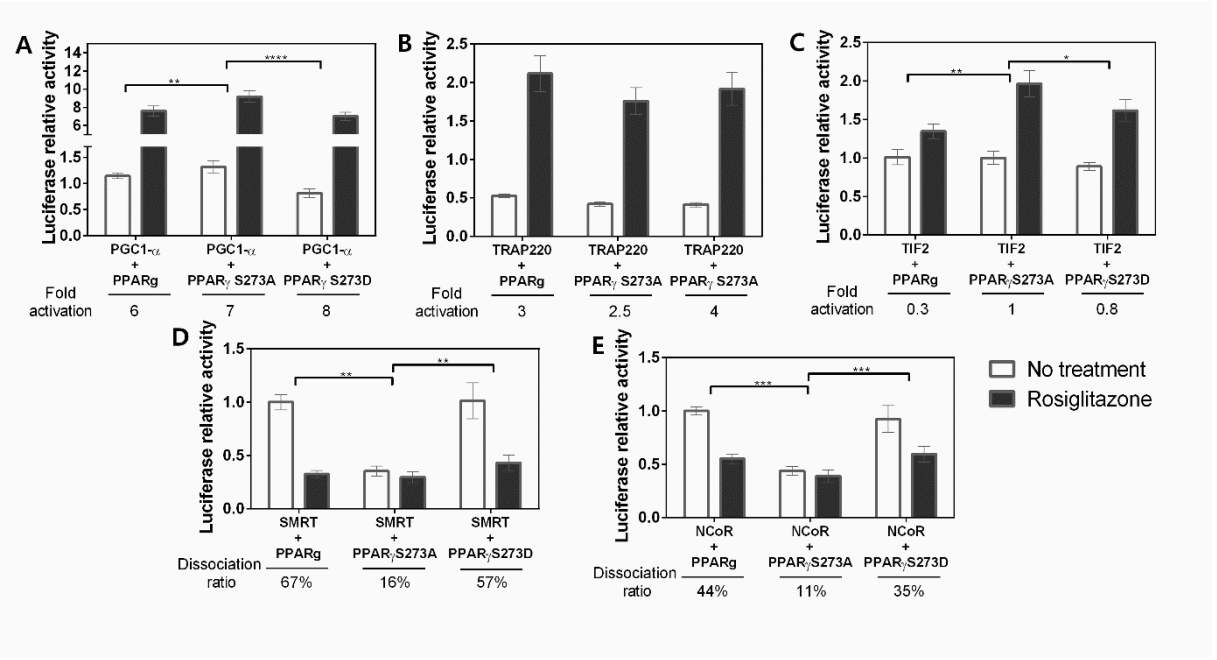

Figure 3 - *Interaction between PPARγ and preferential coregulators in different phosphorylation states*. Affinities measured by mammalian two hybrid assays were performed in COS-7 cells for coactivators and Hek239T cells for corepressors NCoR and SMRT. Error bars, SEM. (n=15) Statistical analysis: two-way ANOVA. p-value: p <0.05 *; p <0.001 *; p <0.001 ***. The coactivators PGC1-α and TIF2 presented elevated interaction with PPARγS273A mutant, while the corepressors presented decreased interaction with the same receptor mutant.

Regarding the corepressors, both were influenced by PPARγ dephosphorylation, as they presented the lowest interaction with S273A mutant (Figures 3D, E), and a decrease in dissociation ratio after Rosiglitazone addition. In contrast, the PPARγ wt and the S273D mutant presented similar interaction activity with corepressors for both SMRT (Figure 3D) and NCoR (Figure 3E), with opposite behavior observed for the coactivator's recruitment. Combined, these results confirm that the phosphorylation inhibition reduces the recruitment of NCoR and SMRT and, at the same time, increases the recruitment of PGC1-α and TIF2.

In addition, these PPARγ:coregulator interactions were confirmed by pull-down assays (Figure 4A). We used tagged coregulator protein as the bait to purify excess of PPARγ and PPARγS273A by affinity chromatography, generating PPARγ:coregulator complexes. Although very useful to confirm the existence of these complexes, this assay did not provide enough accuracy to quantify the differences in affinities between the four coregulators chosen and the different PPARγ

phosphorylation states. However, qualitatively, it is possible to observe that PPARγ binds to all the coregulators in this assay, but the expression of these coregulators in E. coli system is variable in terms of protein content and different affinity comparisons are not possible to perform.

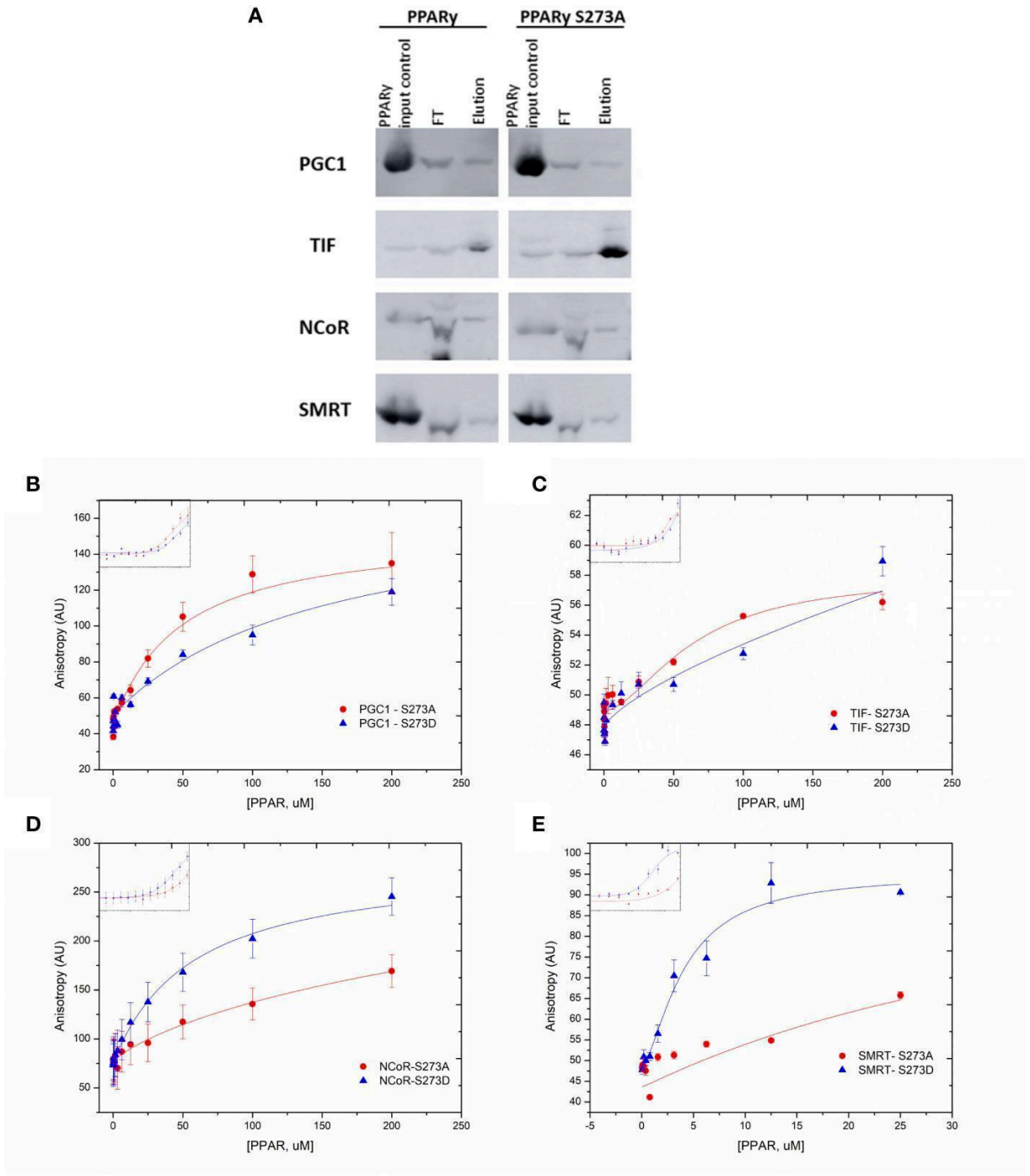

Figure 4 Differential PPARg: coregulator interactions. **(A)** Western blotting analysis of PPARg: coregulator complexes. Tagged coregulators protein extracts were used as bait to bind PPARγ and PPARγS273A by affinity chromatography. The confirmation of complex formation is showed using an antibody against PPARγ in pull-down eluted samples. **(B–E)** Fluorescence anisotropy measurements obtained from the titration of PPARγ wt, S273A and S273D mutants into fluorescein-labeled coregulators. **(B)** PGC1-α anisotropy measurements. **(C)** TIF2 anisotropy measurements. **(D)** NCoR

anisotropy measurements. **(E)** SMRT anisotropy measurements. The experimental controls and kd values are in Supplementary Material.

To confirm these differential interactions, we performed a fluorescence anisotropy assay within the coregulators responsive to S273 phosphorylation (Figures 4B–E). In this assay, coregulators were expressed in E. coli, purified by affinity column, and labeled with FITC. Our results show that PGC1-α binds better to the S273A mutant (Figure 4B) (Kd = 46.9 ± 10) in comparison to the S273D mutant (Kd = 153.5 ± 44.4, respectively), confirming our previous results (Figure 3A). TIF2 presented very low affinities to binding to all the PPARs, which is reflected by the low amplitude of the anisotropy binding curve and by Kds not determined because curves did not achieve saturation (Figure 4C); this result confirms that shown in two-hybrid assays (Figure 2A). Besides this, a preference for the S273 mutant is suggested due to the binding curve shape. Both corepressors presented better affinities with phosphomimetic mutant S273D (Figures 4D, E), and, as also shown in two-hybrid assays, SMRT presented better affinity in comparison to PGC-1 (Kd = 4.06 ± 1.01 uM, and Kd = 55.8 ± 2.9 uM). Together, these data demonstrate strong binding preferences among PPAR mutants, which confirms our two-hybrid assays (Figure 3) results. It is important to mention that this is the first time that bigger constructions of coregulators were assayed in this kind of fluorescence assay, while the most common data about this kind of interaction is presented in the literature using the ID peptides of these molecules. Despite that, the KDs may not be compared to the found ones.

The Phosphorylation State Alters Adipogenesis Profile but Not Necessarily Coregulators Gene Expression

To investigate whether the differential coupling of coregulators is due to differential protein recruitment or changes in coregulators' gene expression, we performed gene expression analysis on differentiated 3T3L1 cells (Figure 5). The cells were treated with Rosiglitazone, a PPARγ agonist, known for increasing its adipogenic capacity [43] and for PPARγ phosphorylation inhibition [44]; with Roscovitine, a CKD5 inhibitor that has already been shown to significantly suppress CDK5-mediated phosphorylation, improving the expression of most of the genes regulated by PPARγ S273 phosphorylation [45]; and by both ligands. In this assay, the

two compounds were used as a treatment during adipogenesis to evaluate whether CDK5 inhibition phosphorylation capacity would modify the expression profile of the chosen coactivators and the adipogenic capacity of PPARγ.

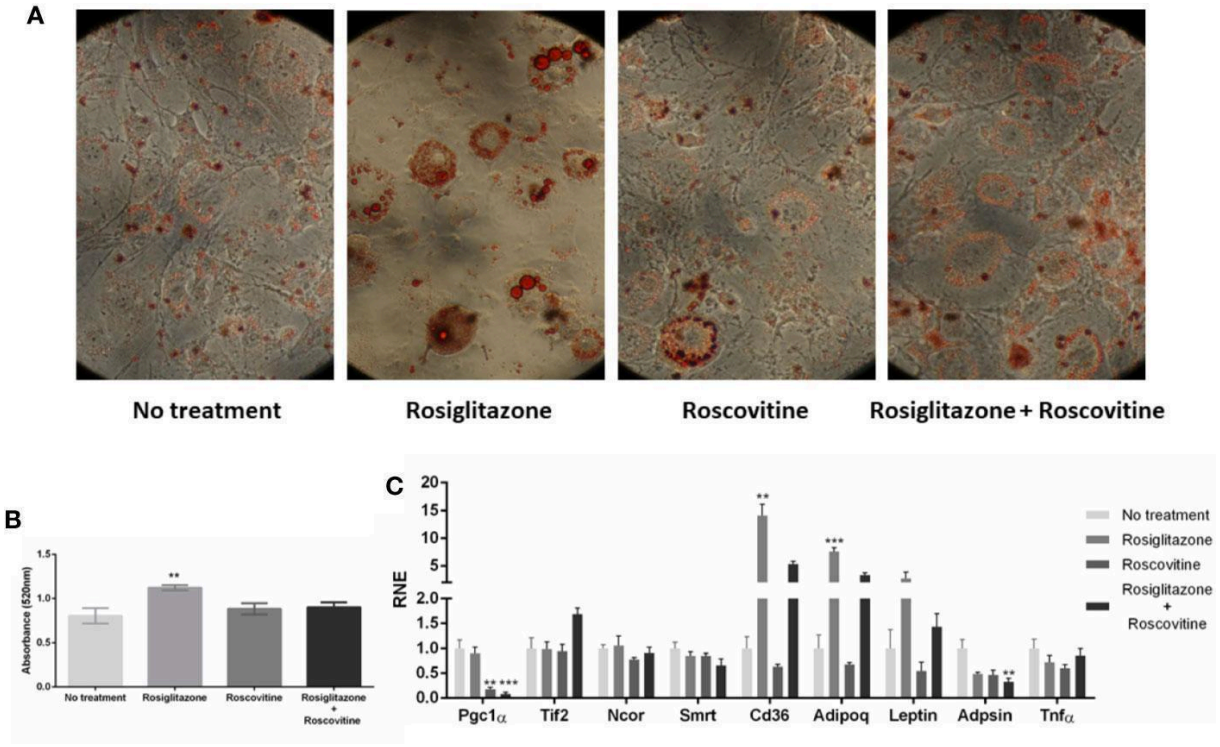

Figure 5 Adipocyte differentiation in different states of PPARγ phosphorylation. **(A)** Images of the 8th day of treatment for differentiation into adipocytes. 3T3-L1 cells after 7 days of treatment with differentiation cocktail stained with Oil Red O in 40× lens. During the differentiation process, 1 μM of Rosiglitazone, 10 μM of Roscovitine, or both treatments were used. **(B)** Absorbance measurement of differentiated cells into adipocytes. After each treatment, the cells were stained with Oil Red O, and a spectrophotometer was used to measure the absorbance. Statistical differences were measured by one-way ANOVA, comparing the different treatments, values of $p < 0.05$/** 0.001/*** 0.001. The treatment with Rosiglitazone showed greater absorbance and, therefore, a higher level of differentiation. **(C)** Gene expression of genes of the studied coregulators and some of the PPARγ regulated genes that were reported to be dysregulated by S273 phosphorylated state (Cd36, Adipoq, Leptin, Adpsin, and Tnf-α). The statistical analysis was performed by the Kruskal-Wallis test (non-parametric), followed by the Dunn post hoc test comparing the untreated condition with each one of the treated conditions. P values: $p \leq 0.01$**; $p \leq 0.001$***.

First, we observed that adipogenesis was reduced in Roscovitine and Roscovitine+Rosiglitazone treatments, as shown in Figures 5A and B. Only Rosiglitazone effectively induced adipocyte differentiation, which is evidenced by the size of the lipid droplets colored by Oil Red O and by the absorbance measurements, suggesting that Roscovitine impairs white adipocyte (WAT) differentiation. As reported, Roscovitine can induce browning of adipose cells, turning the characteristic

bigger lipid droplet in WAT into smaller and multiple lipid droplets that are usual in brown adipose tissue (BAT) [45].

The gene expression results confirm that the differences in PPARγ:coregulators interaction were not due to the differential availability of coregulators in different PPARγ phosphorylation states. Therefore, it confirms the hypothesis of differential interaction profiles that lead to differential activation. Among all the assayed coregulators, we observed a decreased expression of PGC1-α, while TIF-2, NCoR, and SMRT kept the same expression rates in all the treatments. In other words, PGC1-α was the only coregulator downregulated by Roscovitine treatment, even when this compound was associated with Rosiglitazone. Interestingly, as previously shown, the PGC1-α is the PPARγ most recruited coactivator after Rosiglitazone treatment (Figure 2A), and this interaction increased in the absence of PPARγ phosphorylation (Figure 3A). However, CDK5 inhibition seems to decrease this gene expression, suggesting a fine regulation in this coactivator recruitment, which should be specific and strong enough to overpass the limiting expression rates.

Additionally, the other coregulators did not present differences in gene expression rates in all the treatments, suggesting that, for TIF-2, NCoR, and SMRT, changes in PPARγ binding, even in different PPARγ phosphorylation states, are probably caused by different interaction modes, and not due to increased or decreased availability of these proteins. Moreover, we also observed that the PPARγ regulated genes Cd36, Adipoq, and Leptin were upregulated by rosiglitazone, while Rosiglitazone + Roscovitine downregulated Adipsin, and that TNF-α did not change expression profile in all the treatments. These results suggest improved adipogenesis after agonist treatment [43,44], phospho-protective effects against adipogenesis after Roscovitine treatment [45,46], and no inflammation-induced responses in all the conditions, as expected.

IDs Preferences for PPARγ-Coregulator Interaction

Additionally, to identify the preferential binding of PPARγ to each coregulator ID, we performed mammalian two-hybrid assays with coregulators using wt and ID defective constructs of coregulators (Figure 6A) by mutating their active IDs. Hence, the coactivators IDs, with the LXXLL motifs recognized as the ID, had their last two

leucine replaced by alanine residues, resulting in the LXXAA motif. The corepressors domains had the IXX(V/I) motif modified by substituting isoleucine or valine residues for alanine, resulting in the IXXAA motif.

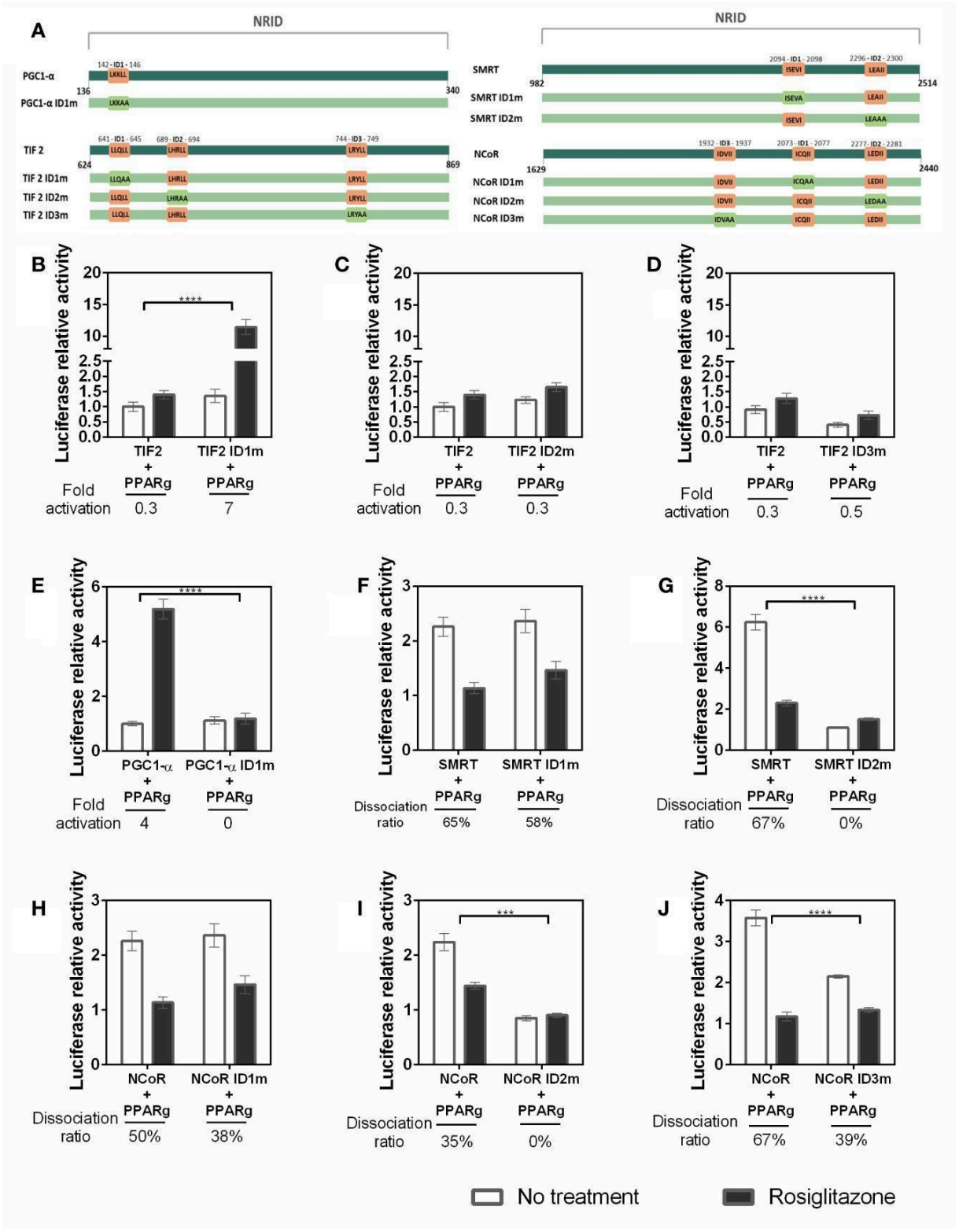

Figure 6 Affinity of the coregulators IDs with PPARγ. **(A)** Representative image of the IDs in the sequences used and their respective mutations. In dark green are the original sequences, and in light

green are the mutated sequences. The original ID sequences are in orange squares, and the mutations in IDs are presented in light green squares. **(B–J)** Mammalian two-hybrid assays were performed to evaluate whether the mutation on each interaction domain (ID) of the coregulators alters the interaction with PPARγ. **(B)** Comparison between interaction with TIF2 coactivator wt and PPARγ, and the ID1 of TIF2 mutated (TIF2 ID1m) and PPARγ. **(C)** ID2 of TIF2 coactivator mutated. **(D)** ID3 of TIF2 coactivator mutated. **(E)** ID1 of PGC1-α coactivator mutated. **(F)** ID1 of SMRT corepressor mutated. **(G)** ID2 of SMRT corepressor mutated. **(H)** ID1 of NCoR corepressor mutated. **(I)** ID2 of the NCoR corepressor mutated. **(J)** ID3 of the NCoR corepressor mutated. Error bars, SEM. (n = 15) Statistical analysis: two-way ANOVA. p-value: P values: $p \leq 0.001$***; $p \leq 0.0001$****. For the TIF coactivator, the withdrawal of ID1 improves the interaction; in this case, we can say that ID1 interferes with the interaction PPARγ-TIF2 and ID3 of the same coactivator is the most important for the interaction. In the case of PGC1-α, we only have 1 ID, and when it is not present, the interaction is broken. For SMRT and NCoR, ID 2 is important, ID1 does not change the interaction, and ID3 of NCoR seems to contribute to the interaction with PPARγ.

Our search for the preferential IDs for PPARγ wt - CoAs binding reveals a panel of ID binding preferences. Firstly, each TIF 2 ID contributes differently to the PPARγ interaction. The ID1 absence (Figure 6B) increased the interaction between TIF2 and PPARγ, indicating that its presence may be disrupting the binding of TIF2 to the PPARγ, possibly by competition between the IDs or unfavorable conformation of the coactivator structure when the ID1 is present (Figures 6C, D). The ID2 mutation (Figure 6C) does not alter the CoA-PPARγ binding, which means that this ID does not contribute to the PPARγ-TIF2 interaction. However, the lack of ID3 (Figure 6D) drastically reduced the interaction with PPARγ, demonstrating that this ID possibly is the most important for PPARγ-TIF2 binding. Concerning PPARγ–PGC1-α binding, the mutation on the unique PGC1-α ID (Figure 6E) decreased the Rosiglitazone-induced interaction with PPARγ, as expected.

We also checked the preferential IDs in the PPARγ wt - CoR binding. Our results show that the lack of SMRT ID1 (Figure 6F) did not provoke any significant differences in the interaction with the receptor, as the efficiency of dissociation of this CoR in the presence of the ligand was also maintained. However, mutation of SMRT ID2 (Figure 6G) reduced the PPARγ-SMRT binding about 6-fold compared with SMRT wt, showing that this ID possibly is the most important in the PPARγ-SMRT interaction. For NCoR, the lack of ID1(Figure 6H) also did not significantly change its interaction with PPARγ, as it was observed for SMRT, but the NCoR ID2 absence (Figure 6I) abolished the PPARγ-NCoR interaction, pointing to the importance of this ID in the corepressor-receptor interaction, as it was also seen for SMRT. Finally, the absence of NCoR ID3 (Figure 6J) decreases the PPARγ-NCoR interaction, but the

reduction found was lower than the found for ID2, suggesting that both ID2 and ID3 contribute to the PPARγ-NCoR interaction, but ID2 is likely the most important one.

The IDs Preferences for PPARγ Binding Change Due to the Phosphorylation State

To evaluate whether the PPARγ S273 phosphorylation state modifies the PPARγ-coregulators interaction profile, we also performed the mammalian two-hybrid assays with the PPARγ S273 mutants and coregulators with IDs mutants. Our results show that changes in TIF2 IDs (Figures 7A–C) presented considerable variation in the interaction with the different PPARγ phosphorylation states. The absence of ID1 (Figure 7A) increased the responsiveness of PPARγ wt to the Rosiglitazone ligand (as shown in Figure 6B and in the first bar of Figure 7A). However, when the phosphorylation is inhibited (PPARγ S273A), the PPARγ-TIF2 interaction decreased, and, in the phosphorylation-mimicking condition (PPARγ S273D), no significant differences between PPARγ wt were observed. Inversely, the absence of ID2 (Figure 7B) increased the interaction of TIF2 with the receptor when the phosphorylation is inhibited (PPARγ S273A) and decreased this interaction with the PPARγ wt and in the phosphorylation mimetic receptor (PPARγ S273D). Mutation on ID3 of TIF2 dramatically decreased receptor interaction under all conditions (Figure 7C). Together, these indicate that the TIF2 ID3 is the most important for the PPARγ interaction, and IDs 1 and 2 are affected by S273 phosphorylation. ID1 may be important to help in the protein-protein interaction for non-phosphorylated PPARγ, and ID2 may be important for the phosphorylated PPARγ interactions.

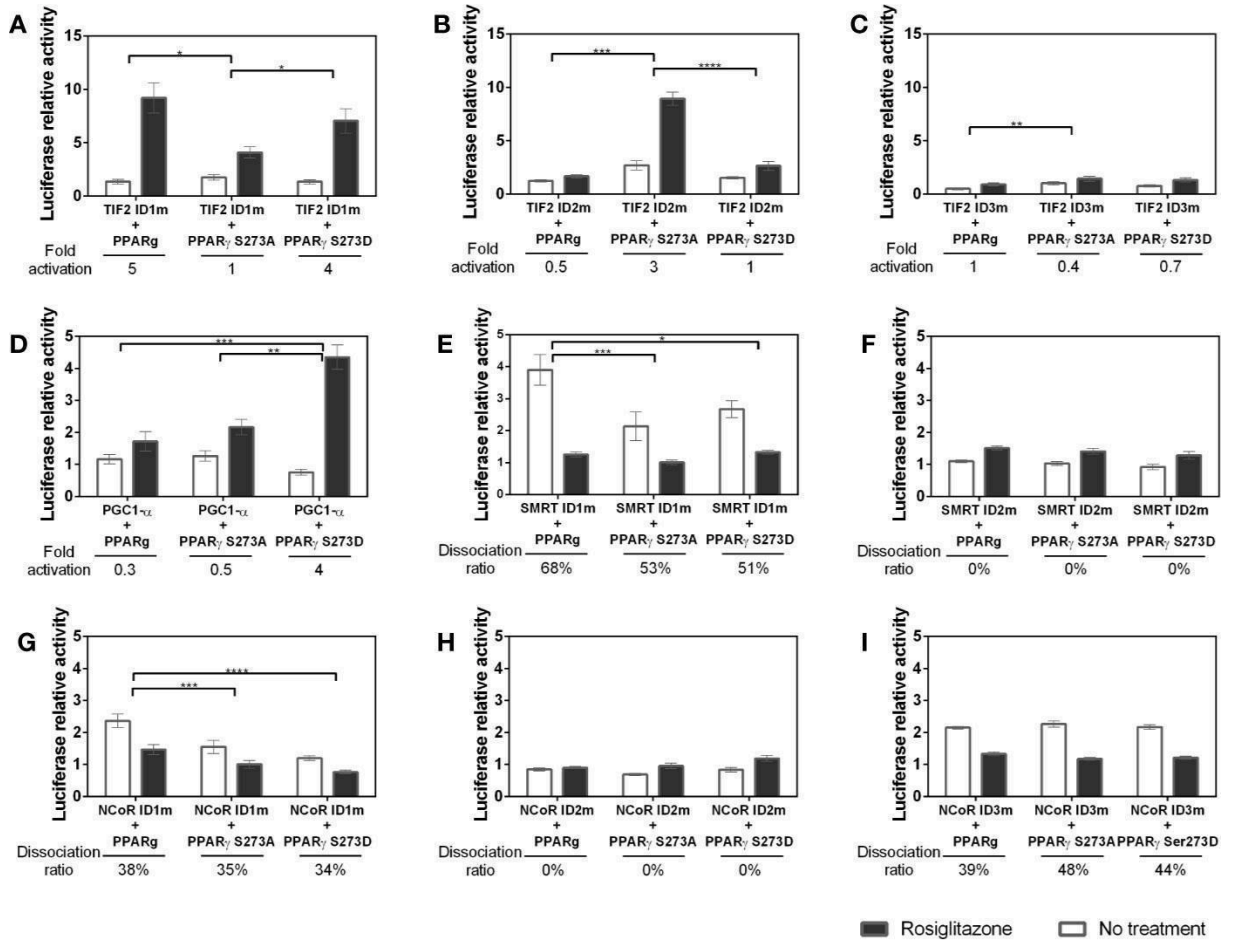

Figure 7 Interaction between coregulators and PPARγ in different phosphorylation states. Mammalian two-hybrid assays were performed to evaluate whether the S273 mutation in the receptor interferes with its interaction with the coregulators. The PPARγ S273A mutant prevents the occurrence of phosphorylation, and the PPARγ S273D mutant is a phosphomimic. **(A–C)** Interaction between TIF2 mutants and PPARγ in different phosphorylation states. **(D)** Interaction between PGC1-α mutant and PPARγ in different phosphorylation states. **(E, F)** Interaction between SMRT mutants and PPARγ in different phosphorylation states. **(G–I)** Interaction between NCoR mutants and PPARγ in different phosphorylation states. Error bars, SEM. (n = 15) Statistical analysis: two-way ANOVA. P values: $p \leq 0.05$*; $p \leq 0.01$**; $p \leq 0.001$***; $p \leq 0.0001$****.

The lack of ID1 in PGC1-α (Figure 7D) shows a similar interaction of this CoA with PPARγ wt and PPARγ S273A. However, phosphorylation (PPARγ S273D) substantially increased the interaction with PPARγ in the presence of ligand, unveiling that this coactivator may bind to an additional receptor region uniquely when it is phosphorylated.

The mutation of SMRT ID1 presented decreased interaction with both conditions of PPARγ mutants (Figure 7E). This suggests that the structural changes provoked by S273 affect the interaction with this ID. The ID2 mutation (Figure 7F) decreased the interaction between PPARγ and SMRT in all phosphorylation states.

This profile was already observed in Figure 6G and is consistent with other studies demonstrating that this is the most important ID for receptor interaction[47,48]. Moreover, no significant difference was observed between the mutation of this ID and PPARγ phosphorylation.

NCoR ID1 mutation (Figure 7G) was also able to reduce the interaction with both mutants, S273A and S273D. Mutation on ID2 (Figure 7H), as the SMRT ID2m, presented a lower interaction with PPARγ in all conditions. The result shows that there is a reduction in the interaction between NCoR with inactive ID2 independent of the state of receptor phosphorylation but due to the PPARγ preference for binding *via* this ID. The ID3 mutation (Figure 7I) showed no difference due to the phosphorylation state, which indicates that this ID is irrelevant in the interaction corepressor-receptor due to phosphorylation/dephosphorylation of PPARγ.

CDK5 Modifies PPARγ-Coregulator Interaction

Finally, to evaluate the preferential coregulator IDs for PPARγ binding and the changes in this preference caused by the receptor's phosphorylation state, we performed some assays in the presence of CDK5 to check if this enzyme would modify the interaction profile with the different coregulators. These assays allow us to estimate what occurs in the cell at the beginning of phosphorylation, while in the previous assays, using S273 mutants, we evaluate the result of phosphorylation in the PPARγ-coregulators binding.

Our results show that PGC1-α, TIF2, and NCoR assays (and D, respectively) decreased receptor interaction in the presence of CDK5. The PGC1-α-PPARγ decreased from 5-fold in the absence of CDK5 to 2-fold. TIF2 decreased PPARγ binding from 1.5-fold to 0.7-fold, indicating that the interaction with the receptor was missed, and NCoR interaction decreased from 4 to 2-fold. Meanwhile, the SMRT corepressor (Figure 8E) displayed the opposite behavior, increasing interaction with PPARγ in the presence of CDK5, indicating that the enzyme may play some roles as PPARγ-corepressor coupling, as previously suggested [33]. Interestingly, for TRAP220, the CDK5 presence did not change the PPARγ-coactivator interaction, as it was shown for the PPARγ mutants. All these results allow us to infer that the enzyme may alter the interaction profile by competing or coupling coregulators to the PPARγ

binding site, depending on the coregulator, and that TRAP is not affected by PPARγ phosphorylation.

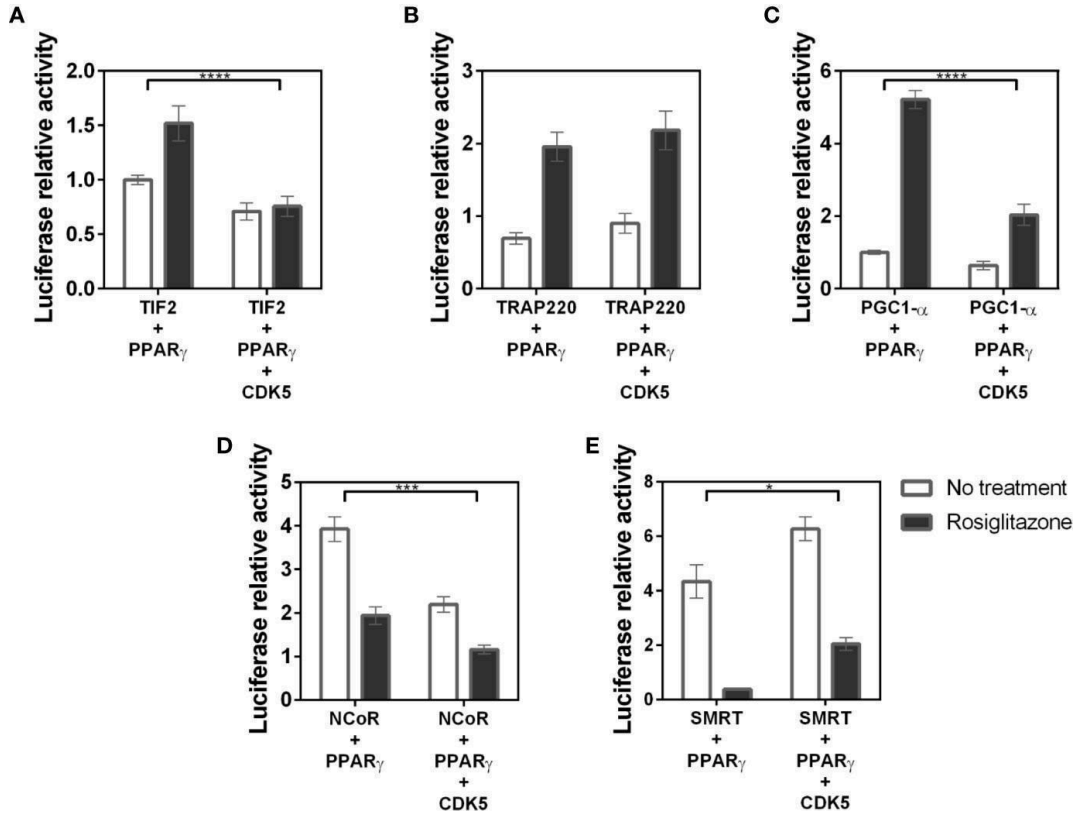

Figure 8 Interaction between coregulators and the PPARγ receptor in the presence of the CDK5 enzyme. Mammalian two hybrid assays to evaluate if the presence of the CDK5 enzyme, responsible for the phosphorylation of S273 in the receptor, interferes with PPARγ:coregulators interaction. **(A)** Interaction of the TIF 2 coactivator with PPARγ in the absence and presence of CDK5. **(B)** Interaction of the TRAP220 coactivator with PPARγ in the absence and presence of CDK5. **(C)** Interaction of the PGC1-α coactivator with PPARγ in the absence and presence of CDK5. **(D)** Interaction of the NCoR corepressor with PPARγ in the absence and presence of CDK5. **(E)** Interaction of the SMRT corepressor with PPARγ in the absence and presence of CDK5. Error bars, SEM. (n = 15) Statistical analysis: two-way ANOVA. P values: $p \leq 0.05$*; $p \leq 0.001$***; $p \leq 0.0001$****. PGC1-α, TIF2 and NCoR showed dissociation of the receptor in the presence of CDK5 while SMRT increased the association with the receptor.

Still, to confirm that CDK5 presence disturbs the PPARγ interaction with coregulators, we perform in vitro phosphorylation assay with heterologously expressed PPARγ and PPARγ-coregulators complexes formed in the pull-down assays (Figure 9). The phosphorylation of PPARγ by CDK5 was used as the control, set up as 100% phosphorylation, and the increase or decrease of the PPARγ phosphorylation due to coregulator presence was compared with this condition. Our results show that the PPARγ:SMRT complex presented an increase of 164% in phosphorylation rate, confirming our cellular assays (Figure 8E) that showed that

CDK5 presence increases SMRT interaction with PPARγ. Moreover, as shown in our cellular assays, the other three complexes presented reduced interaction in CDK5 presence, with PPARγ:PGC1-α complex the one that presented the major interaction disruption, decreasing 52% when added CDK5 in the system. In addition, TIF2 presented a lower interaction difference (11%), possibly due to its weak interaction with PPARγ even in the absence of CDK5. PPARγ:NCoR complex presented a 17% reduction of phosphorylation rate, indicating that NCoR may compete with CDK5-PPARγ for docking.

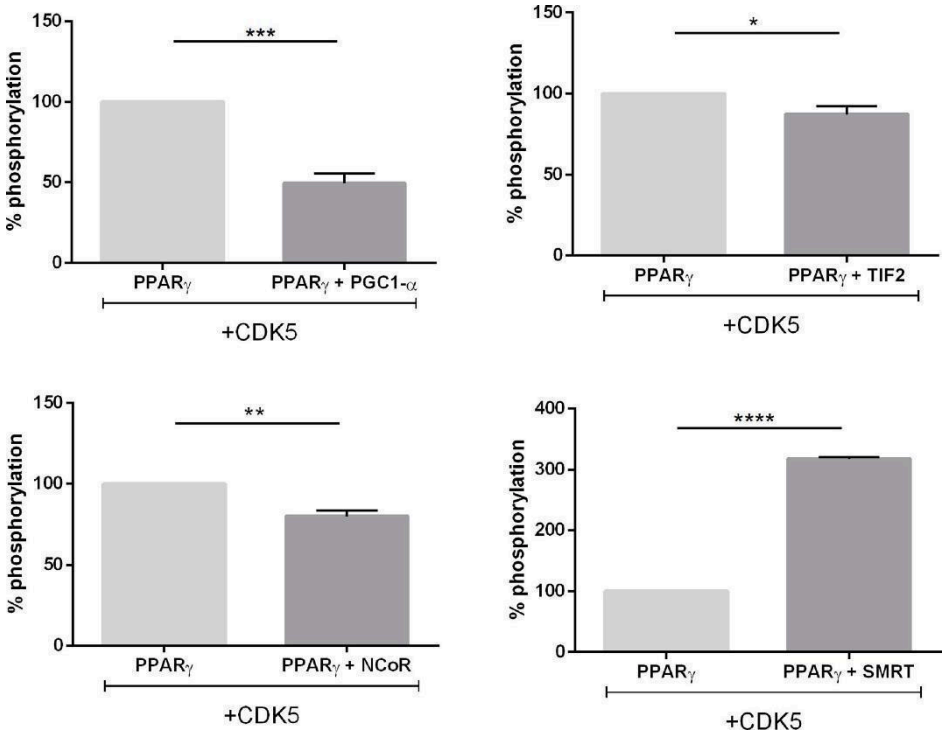

Figure 9 In vitro phosphorylation assay. Luminescence signal produced as a consequence of the ADP production in vitro reaction containing CDK5/p35 kinase, ATP, and PPARγ, and the complexes with coregulators. All the luminescence signals were normalized by PPARγ condition, which is 100% of phosphorylation. Error bars, SEM, (n = 3). Statistical analysis: one-way ANOVA. P values: p ≤ 0.05*; p ≤ 0.01**; p ≤ 0.001***; p ≤ 0.0001****. The complex PPARγ + SMRT presented increased luminescence, while the other three complexes presented decreased luminescence

DISCUSSION

Previous studies have reported that Ser273 phosphorylation of PPARγ LBD is related to obesity-induced development of insulin resistance [44,49,50]. A key question to

understanding the mechanisms of action of this pathway is to elucidate how this phosphorylation influences the PPARγ activation. Our results showed that both phosphorylation status and CDK5 presence can indeed alter the PPARγ activation (Figure 1). Moreover, our results show that these differences in activation are due to the differential interaction with coregulator proteins (Figures 2–4).

As it is well known, the formation of protein-protein complexes and subsequent transcriptional regulation completely depends on the structure [51,52]. PTM-dependent interactions occur through structural changes that create binding sites for a range of IDs[51] . Our results showed that PPARγ binding to coregulators occurs and presented different preferences of binding (Figures 3 and 4) that may be modified by phosphorylation. Additionally, our results show that these binding preferences dependent on the PPARγ phosphorylation state are not due to differential expression of the coregulators or guided by the increased availability of a determined coregulator when phosphorylation is suppressed (Figure 5). On the contrary, the decreased expression of PGC1-α when phosphorylation is inhibited did not change the higher preference of the receptor for this coactivatorpgc1[53,54] .

Through cellular assays, we demonstrate that the coactivator TRAP220 was not responsive to Ser 273 phosphorylation nor to the presence of the CDK5 enzyme (Figures 3 and 6). One possible explanation for this lack of responsiveness is that, although it has 3 different IDs, this coactivator probably binds to PPARγ only by the canonical interface formed by PPARγ H12 relocation and H3, H4 and H5, without any other additional interaction. Thus, neither phosphorylation nor CDK5 presence affects the opposite face of the receptor, not affecting the receptor-coactivator interaction. However, TIF2 and PGC1-α coactivators exhibited a different behavior, presenting higher interaction with PPARγ in the phosphorylation-inhibited state (Figure 3).

Additionally, PGC1-α, PPARγ's preferred coactivator [53,54], showed preferential binding to PPARγ wt by its unique ID (Figure 6E). Moreover, this coactivator makes additional contacts with the receptor in the phosphorylated state, as the deletion of ID1 increased the interaction between the PGC1-α and PPARγ S273D (Figure 7D). Possibly, this contact may be mediated by an additional and inverted LXXLL motif that exists between amino acids 210 to 214 of PGC1-α, which has been shown to interact with other NRs, such as ERRα[55] and is called L3. Despite the fact that it is

well known that the main PGC1-α ID with most NRs is the ID corresponding to L2 (aas 144-149, here called ID1), our results show that when the strongest ID is inactivated, other motifs, as L3 becomes to anchor to the PPARγ, but only if the S273 is phosphorylated. Nevertheless, the existence of this phosphorylation-responsive interaction might explain the decreased interaction of PGC1-α wt with the phosphomimic mutant PPARγ S273D (Figure 3A). In this case, phosphorylation would increase the affinity of L3 motif for the receptor, generating a competition between L2 (or ID1) and L3 motifs, which, for structural reasons, cannot bind at the same time to the receptor, weakening the interaction that was previously made only *via* ID1-H12. This possibly occurs through the CDK5-PGC1-α competition on the PPARγ coupling site. Interestingly, the decreased PGC1-α expression in adipose tissue when such phosphorylation occurs is associated with increased insulin resistance [56].

Interestingly, TIF2, which did not present a high preference to bind PPARγ (Figure 2 and 4C), was also responsive to phosphorylation. Its role in regulating adipose tissue homeostasis and its expression appears to be linked to increased insulin resistance in mice[57]. Our results show it binds to PPARγ canonically *via* ID3 (Figure 6D). However, its other IDs are responsive to phosphorylation in opposite manners. According to our data, ID1 seems to bind better when phosphorylation is inhibited (Figure 7A), but ID2 seems to bind better to the phosphorylated receptor (Figure 7B). This interaction exchange interfaces with the receptor due to its phosphorylation state. It might induce exposure of different interaction surfaces to factors in the transcription activation/repression complex and may lead to different metabolic responses. This type of modular protein ID is used by the cells as a broad device to decode and respond to the state of its protein, with different IDs being dedicated to the selective recognition of distinct PTMs [52].

Regarding corepressors and ID interaction profiles, NCoR and SMRT presented similar behavior. Interestingly, our results showed that there are differences in the recruitment of IDs depending on the corepressor. This difference may be explained by the different mechanisms of binding of the ID1, ID2, and ID3 to the receptor, related to the variants on IDs motifs, which are LXXXIXX (V/I) IXXX (Y/F), LXXIIXXXL, and IXXIIXXXI, respectively [58,59]. Each of them has its own particularities on receptor binding. The ID2, for example, attaches to PPARα by

adopting an irregular three-turn helix that fits tightly into a receptor groove formed by the open conformation of H12. In this case, this surface can also act as a coactivator binding site. Both corepressors showed the strongest interaction with PPARγ *via* ID2, corroborating with previous studies that demonstrate the importance of this ID to PPARγ interaction [47]. On the other side, both ID1 seems to have little or no interaction with PPARγ. However, NCoR ID3 appears responsive to phosphorylation, as the lack of ID1 decreased the PPARγ binding in phosphorylated and no phosphorylated state, and the absence of ID3 did not respond to phosphorylation (Figure 7). This NCoR ID3 response to phosphorylation suggests that possible alternative contacts might be formed between this NCoR ID and the S273 region, as the S replacement for A or D amino acids might provoke particular conformational modifications in PPARγ structure. Interestingly, although the used isoform of SMRT does not have the ID3, the same responsiveness to the phosphorylation was observed since the lack of ID1 also decreased PPARγ interaction when S273 is mutated.

Furthermore, our results revealed that the CDK5 presence also disturbs the PPARγ-coregulators interaction in different ways. Possibly, the CDK5 has some coupling interface with PPARγ that overlaps the interaction interface with the coregulators, as it seems to compete with TIF2, PGC1-α, and NCoR (Figure 8). However, the interaction of PPARγ with SMRT is increased in the presence of CDK5, suggesting that, in this case, it is somehow coupling this corepressor through an interaction interface intersection. These results were confirmed by *in vitro* phosphorylation assays where the complexes TIF2:PPARγ, PGC1-α:PPARγ, and NCoR: PPARγ presented increased ADP activity, and SMRT: PPARγ presented the opposite profile (Figure 9).

This study adds details to the mechanisms of obesity induced by PPARγ phosphorylation. Our data confirm that the coregulators' interaction profile could change due to this phosphorylation[33,60] but also shows that this PTM could lead to new interaction sites within coregulators PPARγ and coregulators CDK5. A better understanding of this mechanism of action opens new pathways for anti-diabetic drug development. Previous studies show that there is a range of molecules that can bind to PPARγ, preventing Ser273 phosphorylation without causing the high activation characteristic of strong agonists [44,61–63] and these results opened a new target

possibility, the PPARγ:coregulator interaction. Inhibitors of this interaction can act either by binding to the binding groove formed by the IDs or by binding to the receptor's H12 [64]. Moreover, our results showed that in addition to these interaction sites, other unusual regions may have their interaction induced by the PPARγ phosphorylation state, further opening the range of possibilities for the new molecules searching.

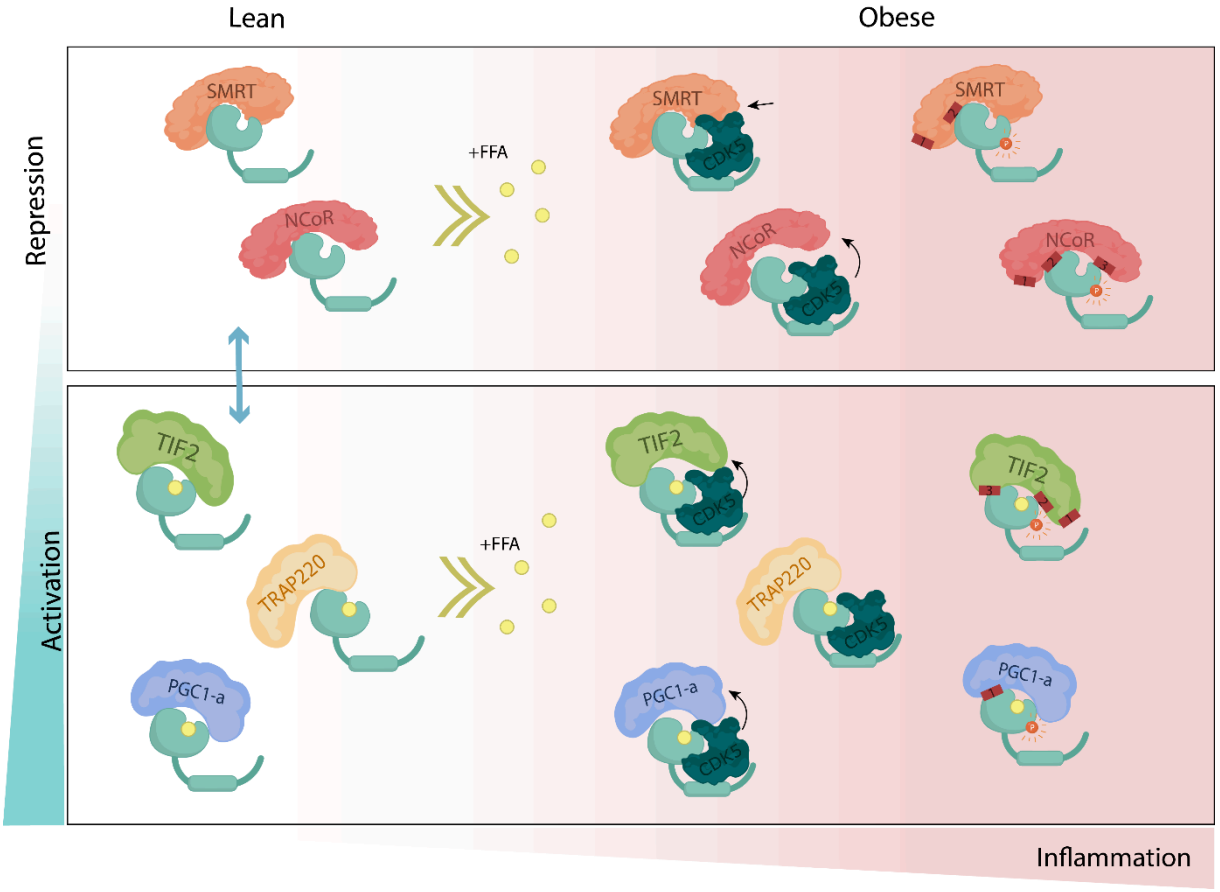

Figure 10 Proposed interaction mechanism. In lean adipose tissue, the mechanism of interaction with coactivators and corepressors is in equilibrium, as represented by the blue arrow. Under conditions of obesity, free fatty acids and other inflammatory factors act by activating the enzyme CDK5 that phosphorylates PPARγ. The presence of CDK5 generates an imbalance in the coregulator's homeostasis, increasing the interaction of PPARγ with SMRT while decreasing with NCoR, PGC1-α, and TIF2. Ser273 phosphorylation performed by CDK5 also modulates the interaction with coregulators. Both corepressors canonically bind *via* ID2-H12 and respond to modification in Ser273, both in the absence and presence of phosphorylation. PGC1-α, although interacting more strongly with the receptor *via* ID1, showed to make additional contact in a region near Ser273 that is favored in the presence of the ligand. TIF2 binds to H12 *via* ID3. However, ID2 seems to interact better in the absence of phosphorylation, and ID1 seems to interact better in the phosphorylation condition. TRAP 220 does not make contact near Ser 273, so it was not responsive to phosphorylation or the presence of CDK5. Red represents the intensity of inflammation in adipose tissue. Blue represents levels of PPARγ activation due to interaction with the coregulators. The numbers 1, 2, and 3 represent the IDs (Created with BioRender.com).

Based on our results, we build a panel of possible PPARγ:coregulators interactions in different phosphorylation states (Figure 10). In summary, we showed that the phosphorylation inhibition increases PPARγ activation through higher interaction with PGC1-α and TIF2 coactivators and decreased interaction with SMRT and NCoR corepressors. The coregulator mutation assay results provide us insights to elucidate the importance of phosphorylation for the different coregulator anchorage possibilities. In particular, our results show that the PGC1-α has been shown to make additional non-ID mediated contact with PPARγ in the region near Ser273. The ID3 of the TIF2 coactivator seems to be the most important for canonical binding via H12, and IDs 1 and 2 make some contacts in the region near Ser273, depending on the phosphorylation state. Both tested corepressors showed that ID2 is the most important for the canonical interaction with PPARγ. However, ID1 is important in cases where modification of receptor S273 occurs, regardless of the receptor phosphorylation state. Finally, we have shown that the presence of CDK5 disrupts interaction with PGC-α, TIF2, and NCoR, probably through competition for the coupling site. In the meantime, the interaction with SMRT increases in this condition. These two different profiles of interaction indicate that the presence of CDK5 imbalances the coregulator's natural activity.

DATA AVAILABILITY STATEMENT

The authors will make the raw data supporting this article's conclusions available without undue reservation.

AUTHOR CONTRIBUTIONS

AF designed the research and article and revised it. MD, TT, FB, HR, FT, AO, and LS performed the research. AM provided essential material and discussed the results and methodology. MD and AF wrote the article. All authors contributed to the article and approved the submitted version.

FUNDING

This work was supported by the “Fundação de Amparo à Pesquisa do Estado de São Paulo” (FAPESP) (grant #2016/22246-0, #2019/14465-1, and #2016/13480-9);

“Conselho Nacional de Desenvolvimento Científico e Tecnológico” (CNPq) (#420416/2016-1); “Coordenação de Aperfeiçoamento de Pessoal de Nível Superior” (CAPES) (grant #88882.329749/2019-01 and #8887.373113/2019-00), and CNPEM.

CONFLICT OF INTEREST

The authors declare that the research was conducted without any commercial or financial relationships that could potentially create a conflict of interest.

ACKNOWLEDGMENTS

We thank the Brazilian Biosciences National Laboratory (LNBio)/ CNPEM for accessibility to the Protein Purification Laboratory (LPP), the Spectroscopy and Calorimetry (LEC), and the Bioassay Laboratory (LBE) facilities. We are grateful to Rafael Cagliari for providing us with CDK5/p25 protein. We also thank to Fundação de Amparo à Pesquisa do Estado de São Paulo – FAPESP, Conselho Nacional de Desenvolvimento Científico e Tecnológico - CNPq, Coordenação de Aperfeiçoamento de Pessoal de Nível Superior – Capes, CNPEM, and LNBio for financial support.

REFERENCES

1 R. M. Evans, G. D. Barish and Y. X. Wang, Nat Med, 2004, 10, 355–361.
2 R. K. Semple, V. K. K. Chatterjee and S. O. Rahilly, Journal of clinical investigation, 2006, 116, 581–589.
3 B. Grygiel-Górniak, Nutr J, , DOI:10.1186/1475-2891-13-17.
4 A. Vidal-Puig, M. Jimenez-Liñan, B. B. Lowell, A. Hamann, E. Hu, B. Spiegelman, J. S. Flier and D. E. Moller, Journal of Clinical Investigation, 1996, 97, 2553–2561.
5 H. P. Guan, T. Ishizuka, P. C. Chui, M. Lehrke and M. A. Lazar, Genes Dev, 2005, 19, 453–461.
6 R. S. Savkur and T. P. Burris, The Journal of Peptide Research, 2004, 63, 207–212.
7 S. Yu and J. K. Reddy, Biochim Biophys Acta Mol Cell Biol Lipids, 2007, 1771, 936–951.

8 R. Brunmeir and F. Xu, International Journal of Molecular Sciences 2018, Vol. 19, Page 1738, 2018, 19, 1738.
9 M. Ahmadian, J. M. Suh, N. Hah, C. Liddle, A. R. Atkins, M. Downes and R. M. Evans, Nat Med, 2013, 99, 557–566.
10 R. Brunmeir and F. Xu, Int J Mol Sci, , DOI:10.3390/ijms19061738.
11 T.-H. Kim, M.-Y. Kim, S.-H. Jo, J.-M. Park and Y.-H. Ahn, Yonsei Med J, 2013, 54, 545–559.
12 M. Adams, M. J. Reginato, D. Shao, M. A. Lazar and V. K. Chatterjee, 1997, 272, 5128–5132.
13 B. Zhang, J. Berger, G. Zhou, A. Elbrecht, S. Biswas, S. White-carrington, D. Szalkowski and D. E. Moller, J Biol Chem, 1996, 271, 31771–31775.
14 S. Choi, J. E. Jung, Y. R. Yang, E. S. Kim, H. J. Jang, E. K. Kim, I. S. Kim, J. Y. Lee, J. K. Kim, J. K. Seo, J. M. Kim, J. Park, P. G. Suh and J. H. Choi, Cell Signal, 2015, 27, 2488–2495.
15 M. Adams, M. J. Reginato, D. Shao, M. A. Lazar and V. K. Chatterjee, 1997, 272, 5128–5132.
16 B. Zhang, J. Berger, G. Zhou, A. Elbrecht, S. Biswas, S. White-carrington, D. Szalkowski and D. E. Moller, J Biol Chem, 1996, 271, 31771–31775.
17 E. Compe, P. Drane, C. Laurent, K. Diderich, C. Braun, J. H. J. Hoeijmakers and J.-M. Egly, Mol Cell Biol, 2005, 25, 6065–6076.
18 I. Iankova, R. K. Petersen, J. S. Annicotte, C. Chavey, J. B. Hansen, I. Kratchmarova, D. Sarruf, M. Benkirane, K. Kristiansen and L. Fajas, Molecular Endocrinology, 2006, 20, 1494–1505.
19 B. Grimaldi, M. M. Bellet, S. Katada, G. Astarita, J. Hirayama, R. H. Amin, J. G. Granneman, D. Piomelli, T. Leff and P. Sassone-Corsi, Cell Metab, 2010, 12, 509–520.
20 D. Shao, S. M. Rangwala, S. T. Bailey, S. L. Krakow, M. J. Reginato and M. A. Lazar, Nature, 1998, 396, 377–380.
21 A. S. Banks, F. E. McAllister, J. P. G. Camporez, P. J. H. Zushin, M. J. Jurczak, D. Laznik-Bogoslavski, G. I. Shulman, S. P. Gygi and B. M. Spiegelman, Nature, 2015, 517, 391–395.
22 J. H. Choi, A. S. Banks, J. L. Estall, S. Kajimura, P. Boström, D. Laznik, J. L. Ruas, M. J. Chalmers, T. M. Kamenecka, M. Blüher, P. R. Griffin and B. M. Spiegelman, Nature, 2010, 466, 451–456.
23 J. H. Choi, A. S. Banks, T. M. Kamenecka, S. A. Busby, M. J. Chalmers, N. Kumar, D. S. Kuruvilla, Y. Shin, Y. He, J. B. Bruning, D. P. Marciano, M. D. Cameron, D. Laznik, M. J. Jurczak, S. C. Schürer, D. Vidović, G. I. Shulman, B. M. Spiegelman and P. R. Griffin, Nature, 2011, 477, 477–481.
24 A. A. Amato, S. Rajagopalan, J. Z. Lin, B. M. Carvalho, A. C. M. Figueira, J. Lu, S. D. Ayers, M. Mottin, R. L. Silveira, P. C. T. Souza, R. H. V Mour??o, M. J. A. Saad, M. Togashi, L. A. Simeoni, D. S. P. Abdalla, M. S. Skaf, I. Polikparpov, M. C. A. Lima, S. L. Galdino, R. G. Brennan, J. D. Baxter, I. R. Pitta, P. Webb, K. J. Phillips and F. A. R. Neves, Journal of Biological Chemistry, 2012, 287, 28169–28179.

25 S. S. Choi, E. S. Kim, M. Koh, S. J. Lee, D. Lim, Y. R. Yang, H. J. Jang, K. A. Seo, S. H. Min, I. H. Lee, S. B. Park, P. G. Suh and J. H. Choi, Journal of Biological Chemistry, 2014, 289, 26618–26629.
26 C. Liu, T. Feng, N. Zhu, P. Liu, X. Han, M. Chen, X. Wang, N. Li, Y. Li, Y. Xu and S. Si, Sci Rep, 2015, 5, 9530.
27 X. Xie, X. Zhou, W. Chen, L. Long, W. Li, X. Yang, S. Li and L. Wang, Biochimica et Biophysica Acta (BBA) - General Subjects, 2015, 1850, 62–72.
28 W. Zheng, L. Qiu, R. Wang, X. Feng, Y. Han, Y. Zhu, D. Chen, Y. Liu, L. Jin and Y. Li, Sci Rep, 2015, 5, 12222.
29 H. V. R. Filho, N. B. Videira, A. V. Bridi, F. A. H. B. Thais Helena Tittanegro, J. G. de Carvalho, Pereira, P. S. L. de Oliveira, M. C. Bajgelman, A. Le Maire and A. C. M. Figueira, , DOI:10.3389/fendo.2018.00011.
30 H. V. Ribeiro Filho, J. V. Guerra, R. Cagliari, F. A. H. Batista, A. Le Maire, P. S. L. Oliveira and A. C. M. Figueira, J Struct Biol, 2019, 207, 317–326.
31 O. Hermanson, C. K. Glass and M. G. Rosenfeld, 2002, 13, 55–60.
32 J. H. Choi, S. S. Choi, E. S. Kim, M. P. Jedrychowski, Y. R. Yang, H. J. Jang, P. G. Suh, A. S. Banks, S. P. Gygi and B. M. Spiegelman, Genes Dev, , DOI:10.1101/gad.249367.114.
33 P. Li, W. Fan, J. Xu, M. Lu, H. Yamamoto, J. Auwerx, D. D. Sears, S. Talukdar, D. Oh, A. Chen, G. Bandyopadhyay, M. Scadeng, J. M. Ofrecio, S. Nalbandian and J. M. Olefsky, Cell, 2011, 147, 815–826.
34 C. Yu, K. Markan, K. A. Temple, D. Deplewski, M. J. Brady and R. N. Cohen, Journal of Biological Chemistry, 2005, 280, 13600–13605.
35 S. R. Farmer, 2006, 263–273.
36 G. Medina-gomez, S. Gray and A. Vidal-puig, 2007, 10, 1132–1137.
37 A. Koppen and E. Kalkhoven, FEBS Lett, 2010, 584, 3250–3259.
38 N. Dissmeyer and A. Schnittger, Guide to the book plant kinases, 2011, vol. 779.
39 J. Fattori, N. de C. Indolfo, J. C. L. de O. Campos, N. B. Videira, A. V. Bridi, T. R. Doratioto, M. A. de Assis and A. C. M. Figueira, Nucl Receptor Res, 2014, 1, 1–20.
40 A. Le Maire, C. Teyssier, C. Erb, M. Grimaldi, S. Alvarez, A. R. De Lera, P. Balaguer, H. Gronemeyer, C. A. Royer, P. Germain and W. Bourguet, Nat Struct Mol Biol, 2010, 17, 801–807.
41 E. M. Phizicky and S. Fields, Microbiol Rev, 1995, 59, 94–123.
42 C. M. Tyree and K. Klausing, Methods Mol Med, 2003, 85, 175–83.
43 M. J. Nanjan, M. Mohammed, B. R. Prashantha Kumar and M. J. N. Chandrasekar, Bioorg Chem, 2018, 77, 548–567.
44 J. H. Choi, A. S. Banks, J. L. Estall, S. Kajimura, P. Boström, D. Laznik, J. L. Ruas, M. J. Chalmers, T. M. Kamenecka, M. Blüher, P. R. Griffin and B. M. Spiegelman, Nature, 2010, 466, 451–456.
45 H. Wang, L. Liu, J. Z. Lin, T. R. Aprahamian and S. R. Farmer, Cell Metab, 2016, 24, 835–847.
46 X. Hu, Y. Li and M. A. Lazar, Mol Cell Biol, 2001, 21, 1747–1758.

47 S. M. Reilly, P. Bhargava, S. Liu, M. R. Gangl, C. Gorgun, R. R. Nofsinger, R. M. Evans, L. Qi, F. B. Hu and C. H. Lee, Cell Metab, 2010, 12, 643–653.
48 X. Hu, Y. Li and M. A. Lazar, Mol Cell Biol, 2001, 21, 1747–1758.
49 S. Choi, J. E. Jung, Y. R. Yang, E. S. Kim, H. J. Jang, E. K. Kim, I. S. Kim, J. Y. Lee, J. K. Kim, J. K. Seo, J. M. Kim, J. Park, P. G. Suh and J. H. Choi, Cell Signal, 2015, 27, 2488–2495.
50 J. H. Choi, A. S. Banks, T. M. Kamenecka, S. A. Busby, M. J. Chalmers, N. Kumar, D. S. Kuruvilla, Y. Shin, Y. He, J. B. Bruning, D. P. Marciano, M. D. Cameron, D. Laznik, M. J. Jurczak, S. C. Schürer, D. Vidović, G. I. Shulman, B. M. Spiegelman and P. R. Griffin, Nature, 2011, 477, 477–481.
51 E. Yeger-Lotem, S. Sattath, N. Kashtan, S. Itzkovitz, R. Milo, R. Y. Pinter, U. Alon and H. Margalit, Proc Natl Acad Sci U S A, 2004, 101, 5934–5939.
52 B. T. Seet, I. Dikic, M. M. Zhou and T. Pawson, Nature Reviews Molecular Cell Biology 2006 7:7, 2006, 7, 473–483.
53 P. Puigserver, Z. Wu, C. W. Park, R. Graves, M. Wright and B. M. Spiegelman, Cell, 1998, 92, 829–839.
54 D. Knutti and A. Kralli, Trends in Endocrinology and Metabolism, 2001, 12, 360–365.
55 S. N. Schreiber, D. Knutti, K. Brogli, T. Uhlmann and A. Kralli, Journal of Biological Chemistry, 2003, 278, 9013–9018.
56 A. Hammarstedt, P. A. Jansson, C. Wesslau, X. Yang and U. Smith, Biochem Biophys Res Commun, 2003, 301, 578–582.
57 F. Picard, M. Géhin, J. S. Annicotte, S. Rocchi, M. F. Champy, B. W. O'Malley, P. Chambon and J. Auwerx, Cell, 2002, 111, 931–941.
58 C. Guo, Y. Li, C. H. Gow, M. Wong, J. Zha, C. Yan, H. Liu, Y. Wang, T. P. Burris and J. Zhang, Journal of Biological Chemistry, 2015, 290, 3666–3679.
59 A. Le Maire, C. Teyssier, C. Erb, M. Grimaldi, S. Alvarez, A. R. De Lera, P. Balaguer, H. Gronemeyer, C. A. Royer, P. Germain and W. Bourguet, Nature Structural & Molecular Biology 2010 17:7, 2010, 17, 801–807.
60 J. H. Choi, S. S. Choi, E. S. Kim, M. P. Jedrychowski, Y. R. Yang, H. J. Jang, P. G. Suh, A. S. Banks, S. P. Gygi and B. M. Spiegelman, Genes Dev, 2018, 28, 2361–2369.
61 S. S. Choi, E. S. Kim, M. Koh, S. J. Lee, D. Lim, Y. R. Yang, H. J. Jang, K. A. Seo, S. H. Min, I. H. Lee, S. B. Park, P. G. Suh and J. H. Choi, J Biol Chem, 2014, 289, 26618–26629.
62 S. S. Choi, E. S. Kim, M. Koh, S. J. Lee, D. Lim, Y. R. Yang, H. J. Jang, K. A. Seo, S. H. Min, I. H. Lee, S. B. Park, P. G. Suh and J. H. Choi, Journal of Biological Chemistry, 2014, 289, 26618–26629.
63 H. V. R. Filho, N. B. Videira, A. V. Bridi, F. A. H. B. Thais Helena Tittanegro, J. G. de Carvalho, Pereira, P. S. L. de Oliveira, M. C. Bajgelman, A. Le Maire and A. C. M. Figueira, Front Endocrinol (Lausanne), 2018, 9, 1–10.
64 K. J. Skowron, K. Booker, C. Cheng, S. Creed, B. P. David, P. R. Lazzara, A. Lian, Z. Siddiqui, T. E. Speltz and T. W. Moore, Mol Cell Endocrinol, 2019, 493, 110471.

3. DOCUMENTO EM SUBMISSÃO

3.1. Artigo II - S273 phosphorylation restricts PPARγ structural dynamics - a multiscale modeling view on the Mechanisms of Obesity Metabolism

Open Access Published: 23 October 2024. doi: https://doi.org/10.26434/chemrxiv-2024-j57mx

Author names and affiliations:

Marieli Mariano Gonçalves Dias[1,2,3], Cristina Gil Hererro[2], Ana Carolina Migliorini Figueira[1*], Sebastian Thallmair[2*]

[1]Brazilian Center for Research in Energy and Materials (CNPEM), Campinas, Brazil.

[2]Frankfurt Institute for Advanced Studies (FIAS), Frankfurt, Germany

[3]Graduate Program in Molecular and Morphofunctional Biology, Institute of Biology, State University of Campinas (Unicamp), Campinas, Brazil.

*Corresponding authors: ana.figueira@lnbio.cnpem.br, thallmair@fias.uni-frankfurt.de

Abstract

The nuclear receptor PPARγ is a promising target for treating type 2 diabetes mellitus. It regulates gene expression related to insulin and lipid metabolism. The obesity-linked phosphorylation of PPARγ S273 disrupts the expression of a specific subset of PPARγ-controlled genes linked to insulin metabolism, such as adiponectin. Previous research has demonstrated that this post-translational modification alters interactions with several coregulators, thereby influencing the expression of upstream genes. However, the effects of phosphorylation on the structural dynamics of PPARγ have not yet been fully understood. In this study, we applied atomistic and coarse-grained molecular dynamics simulations to examine the structural and dynamic changes induced by S273 phosphorylation. We observed that the phosphorylation impacts the dynamics of adjacent residues and influences more distantly located structural regions. Furthermore, S273 phosphorylation alters the flexibility of H12, the region responsible for canonical interaction with coregulators, potentially

accounting for the previously observed differential interactions. These findings provide new insights into the mechanisms of gene expression regulation and may expand the avenues into diabetes therapy studies through PPARγ modulation. Moreover, they highlight the potential of combined atomistic and coarse-grained simulations to elucidate modifications of structural dynamics in proteins upon post-translational modification.

Introduction

The transcription factor Peroxisome Proliferator-Activated Receptor γ (PPARγ) is a master regulator of adipogenesis, governing the expression of lipid and glucose metabolism genes. Upon activation, PPARγ facilitates the differentiation of pre-adipocytes into mature adipocytes and enhances glucose uptake by adipose cells, thereby decreasing insulin resistance and inducing insulin sensitivity through the regulation of its associated genes, such as adipsin and adiponectin[1,2]. Consequently, manipulating PPARγ activation holds promise for enhancing adipocyte glucose uptake, thus potentially ameliorating insulin resistance.

The canonical transcriptional activity of PPARγ occurs through its interaction with coregulator proteins, which either activate or repress gene transcription. In the absence of ligands, the inactive conformation of helix 12 (H12) within the PPARγ ligand binding pocket (LBD) favors the binding of corepressor proteins. In conjunction with histone deacetylases (HDACs), these corepressor proteins form a complex that hinders the transcription of the target gene [3]. Upon binding of an agonist ligand to the LBD, the receptor undergoes a conformational change, resulting in the relocation of H12 and forming a charged clamp between helix H3 and helix H4 [4]. This conformational change induces the dissociation of corepressors and promotes the recruitment of coactivators. These proteins will organize into a coactivator complex with other proteins from the transcription machinery, such as histone acetyltransferases (HAT) and other general transcription factors, ultimately initiating the transcription of the target gene [5].

Besides ligand binding, post-translational modifications (PTMs) can also impact the recruitment of corepressors or coactivators. The S273 phosphorylation of PPARγ is an obesity-linked PTM that disrupts the regular coregulator exchange [6,7]. The phosphorylation is performed by the cyclin-dependent kinase 5 (CDK5) and influences the expression of insulin-sensitizing adipokines such as adiponectin and adipsin [8,9]. Meanwhile, various PPARγ ligands have demonstrated the ability to prevent this phosphorylation event, improving insulin sensitization [10,11]. Interestingly, these ligands do not directly interact with residue S273 (S245 in the γ1 variant) but induce structural alterations in the PPARγ-CDK5 interaction interface, thereby safeguarding the site from phosphorylation [8].

While not affecting the receptor's adipogenic capacity or its occupancy on DNA, S273 phosphorylation induces differential binding to several coregulators, which could explain its selective change in gene expression. In particular, the coactivator Thrap3 directly interacts with PPARγ when S273 is phosphorylated, enhancing the expression of the diabetic genes [7]. Our previous study presented a comprehensive analysis of different coregulators whose interaction with PPARγ is disturbed upon S273 phosphorylation [6]. We demonstrated that inhibition of S273 phosphorylation increased PPARγ’s interaction with the coactivators PGC1-α and TIF2, whereas its interaction with SMRT and NCoR corepressors decreased. Moreover, we found that the phosphorylation caused not the absence of binding but rather a change in the coregulators' interaction domains (IDs) preferences[6].

Coregulator proteins bind selectively to different nuclear receptors through their IDs. The precise orchestration of coregulator binding is crucial, as the initial binding event determines the proteins that will subsequently be recruited, ultimately forming the initial transcription machinery. Consequently, alterations in the preferential region of interaction can lead to changes in the recruitment of the initial transcription machinery, thereby impacting the expression of target genes.

In the present study, we examined how S273 phosphorylation modulates the properties of PPARγ, providing more details about PPARγ’s mechanism of

action. Using computational methods, we investigated how this PTM affects protein dynamics. Our atomistic and coarse-grained (CG) simulations demonstrated that S273 phosphorylation leads to notable mobility changes both in the vicinity of the phosphorylation site as well as in more distant regions. These changes were particularly noteworthy in loop regions such as the Ω loop and 6/7 loop, with consequential effects also observed in H9. Furthermore, our investigation demonstrated that the mobility of H12 is perturbed by the reorganization of molecular interactions in the diphenyl pocket, a region comprising the loops 6/7, 11/12, and H3 [12]. Our results provide a deeper understanding of the structural changes that govern the regulation of gene expression by PPARγ. These insights can potentially serve as a basis to improve diabetes treatment by addressing non-agonism modulation of PPARγ.

Results and Discussion

S273 phosphorylation decreases PPARγ overall flexibility

Despite the phosphorylation of PPARγ S273 being involved in the dysregulation of a subset of genes linked to insulin resistance, its precise mechanism of action is unknown. We conducted CG molecular dynamics (MD) simulations using the Martini 3 force field[13] and Gō-like models[14] to investigate its impact on the structural flexibility of PPARγ. To this end, 10 replicas of 25 μs each were performed for the wild-type (WT) and phosphorylated S273 (PO4) variant of the LBD of PPARγ.

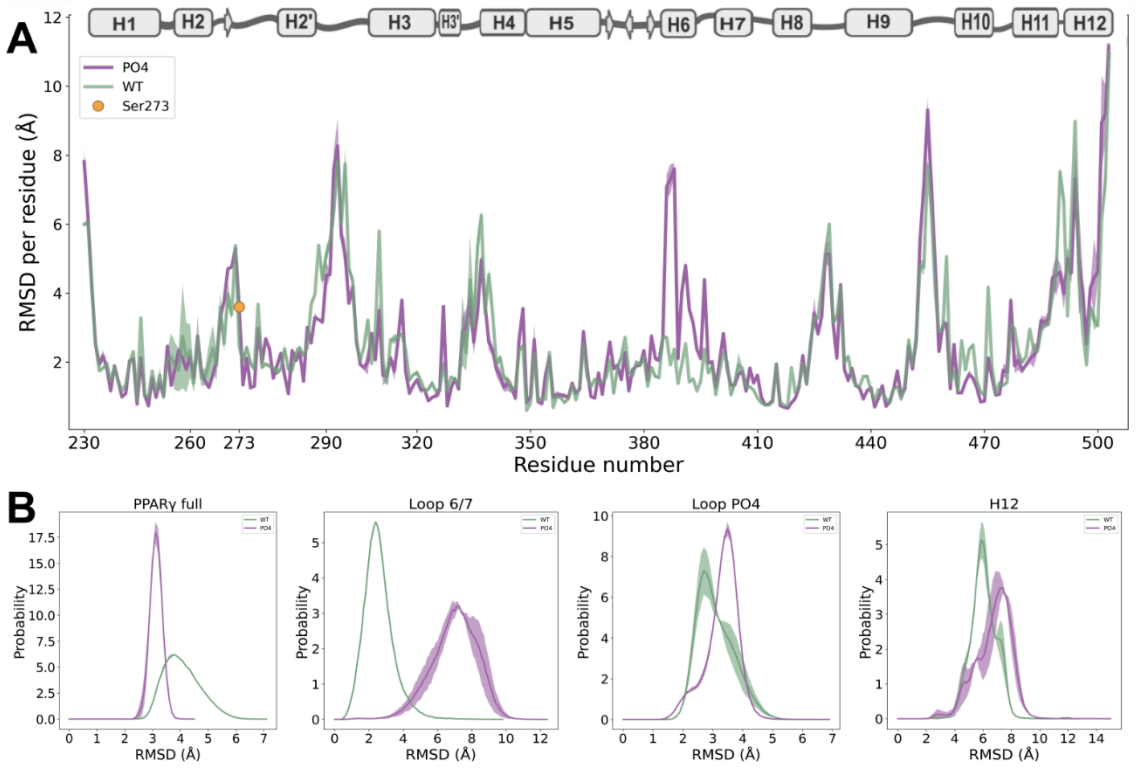

Figure 1—Flexibility analysis of PPARγ LBD. Panel (A) presents the RMSD (Root Mean Square Deviation) per residue of the backbone (BB) beads from the 250 μs trajectories of PPARγ WT (green) and PPARγ S273 phosphorylated (PO4, purple). The orange dot represents the phosphorylated residue. Panel (B) shows RMSD distributions per time of the full protein and of important regions affected by S273 phosphorylation.

Comparing the backbone beads (BB) root mean square deviation (RMSD) (Figure 1), we observed that the phosphorylation induced variable flexibility changes along the protein. While the S273 phosphorylation caused a decrease in the overall protein RMSD (Figure 1B, left), it induced an increase of local flexibility in specific regions, such as the loop 6/7, loop PO4, and H12. Notably, these regions are essential for activation (H12) and ligand binding (loop 6/7, loop PO4).

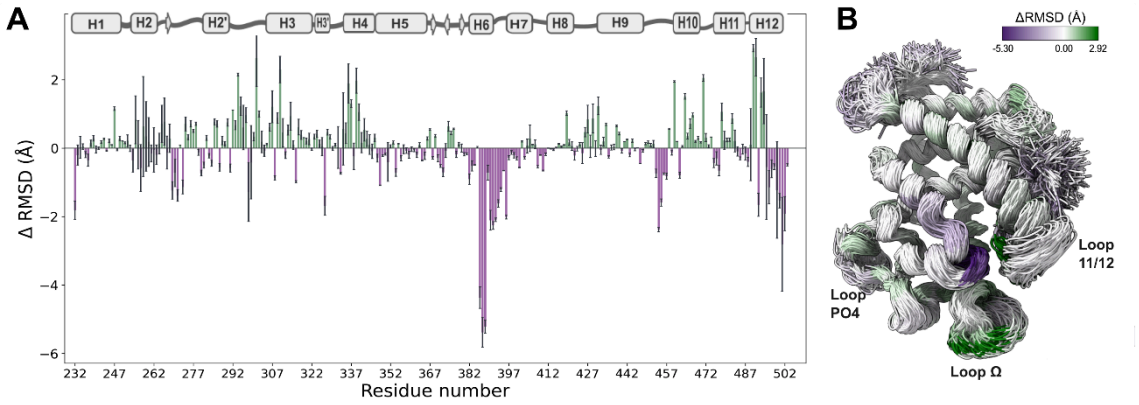

Figure 2 – Comparative analysis of PPARγ LBD residue deviations. (A) Difference between WT and PO4 RMSD values for each residue in PPARγ LBD. Positive values are displayed in green, representing increased flexibility in the WT variant. Negative values, representing a gain of flexibility upon S273 phosphorylation, are displayed in purple. (B) PPARγ LBD structure, colored according to the differences in RMSD. Purple residues indicate a gain in flexibility with S273 phosphorylation, and green indicates flexibility loss when S273 is phosphorylated.

The residues in the 6/7 loop presented the most considerable difference. We also observed higher flexibility at loop 9/10 and the end of H12. Nonetheless, the loop linking H11 to H12, essential for H12's mobility, is more flexible in the PPARγ WT trajectories. The RMSD per residue presented in Figure 1A uncovered the increase in mobility of some key residues at PPARγ LBD due to S273 phosphorylation. Surprisingly, the most affected residues are not structurally close to the phosphorylation site but in distant loop regions, such as loop 6/7, loop 9/10, and the highly flexible H12. The latter is directly responsible for the interaction with coregulators, which may explain the differential interaction previously reported by our group [6].

We compared each residue's BB flexibility in the LBD structure by subtracting the BB RMSD values of the PO4 trajectories from the ones of the WT trajectories (Figure 2). Residues that are more flexible in the WT are colored green, and those that are less flexible in the WT are colored purple, both in the bar graph (A) and the PPARγ LBD structure (B).

Residue 388 has the highest gain in BB mobility upon S273 phosphorylation, with $\Delta RMSD^{WT-PO4} = -5.3$ Å. Also, the neighboring residues 386 and 387, located in the loop 6/7, showed the most pronounced gain in mobility upon S273 phosphorylation (see also Figure S2). Loss of function of these residues is

a known factor associated with familial partial lipodystrophy (FPLD) [15,16]. A mutation of residue 388 leads to decreased basal transcriptional activity and impairing stimulation by synthetic ligands [15], suggesting a role in PPARγ ligand-induced activation. Structural characterization of the F388L mutant showed that this mutation induces the loss of some meaningful interactions that stabilize the loop 11/12, directly impacting the H12 flexibility [16]. Overall, while our data shows mixed trends for the BB flexibility, the overall flexibility, considering the side chains as well, clearly indicates reduced flexibility of the whole protein. However, some important regions of PPARγ, such as loop 6/7, experience an increase in flexibility upon S273 phosphorylation.

S273 phosphorylation stabilizes the diphenyl pocket

An in-depth analysis of the most flexible regions in atomistic MD simulations revealed an intricate contact network at the bottom of the ligand cavity, delimited by the loop 11/12 and flanked by H3 (see Figure 3). In both variants (WT and PO4), non-bonded interactions were observed between residues 484 and 488 in H11 and residues 385 and 388 in the loop 6/7 (Figure 3A). Also, residue 385 in the loop 6/7 interacted with residue 304 in H3, and residue 388 with residues 307 and 310 in H3, overall forming a pocket-like structure. With the phosphorylation at S273, the residue 490 in the loop 11/12 faces this pocket inwards, moving loop 11/12 closer to H3 by establishing non-bonded interactions with residues 303, 307, 385, and 388 (Figure 3B).

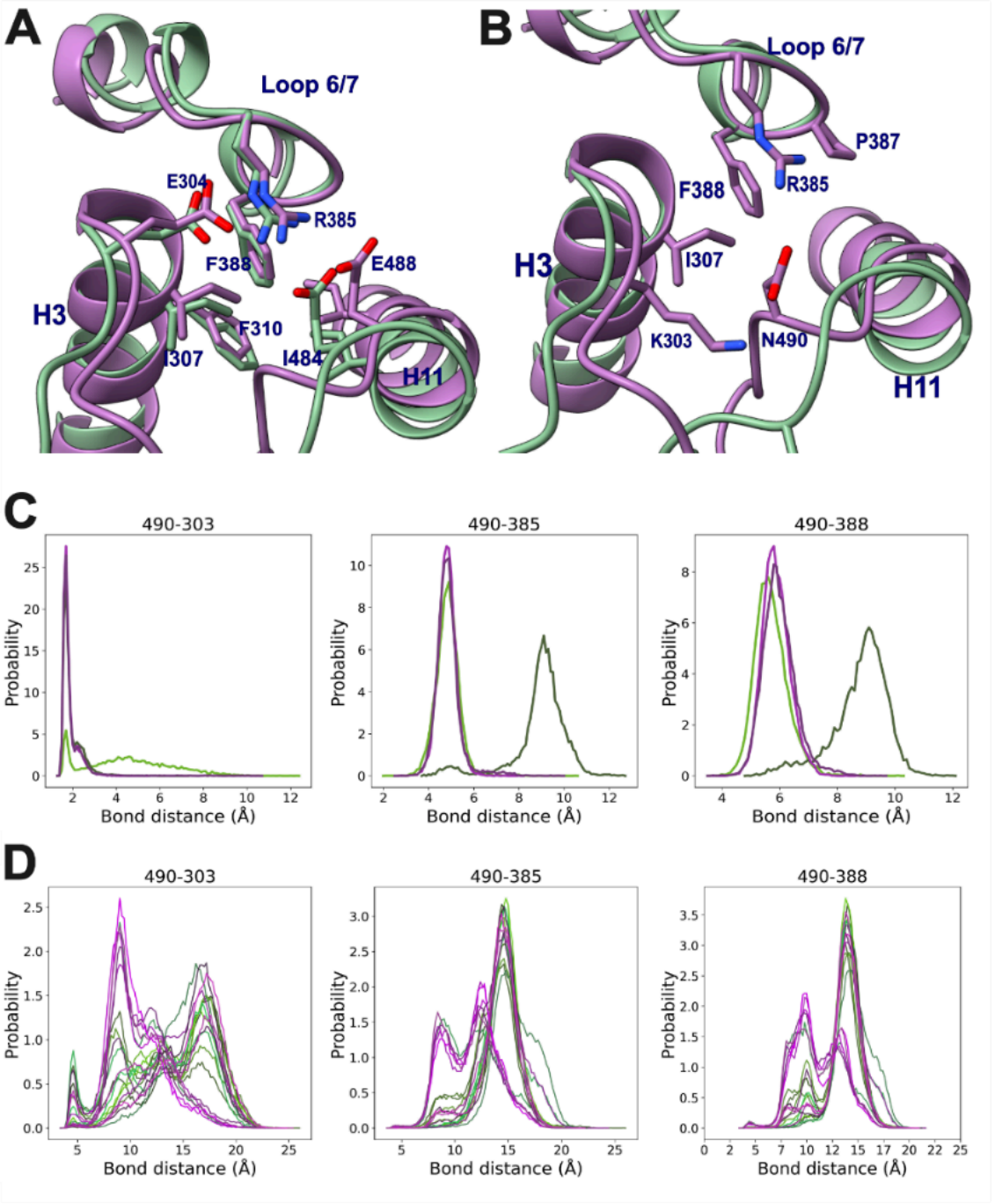

Figure 3 –Differential non-bonded interaction network upon S273 phosphorylation. (A) In atomistic trajectories, shared interaction residues for WT (green) and PO4 (purple) were obtained. (B) New interactions were established in the trajectories of S273 phosphorylated PPARγ. The repositioning of N490 creates new interactions with nearby residues, inducing rigidification of the loop 11/12. (C) Bond distance distributions for selected residue pairs in the atomistic trajectories. Two replicas of 1 μs each were performed for each PPARγ LBD variant. (D) Bond distance distributions for selected residue pairs in the coarse-grained trajectories. Ten replicas of 25 μs each were performed for each PPARγ LBD variant. Note that due to coarse-graining, the distances increase compared to atomistic structures. WT distributions are displayed in green; phosphorylated ones in purple.

The atomistic distance distributions for three of the interactions of residue 490 (Figure 3C) indicate a stabilization of the loop 11/12 due to phosphorylation of S273. In the WT, two meta-stable orientations of N490 were observed, suggesting a flexible non-bonded interaction network. In contrast, in the phosphorylated variant, these same residues exhibited closer and more stable interactions with the N490 residue, giving rise to a coordinated movement that reinforces the non-bonded interactions within the pocket (Figure 3B). The extended simulation time of the CG trajectories enables the protein to explore a larger conformational space, providing a more comprehensive picture (Figure 3D). Note that the absolute distances increase from atomistic to CG resolution due to the nature of coarse-graining; namely, multiple atoms are grouped into larger beads, which increases measured distances between residues in contact. Nevertheless, residue 490 of the WT is indeed more flexible also at CG resolution. The analysis reveals a pattern in the behavior of the PO4 variant, characterized by closer contacts and higher rigidity of some interactions (Figure 3D).

The repositioning of residue 490 into the pocket (Figure 3B) results in a novel interaction network involving residues 303, 307, 385, 387, and 388, which rigidifies the bottom part of the ligand pocket. This new interaction network rearranges loops 6/7 and 11/12 and keeps H3 and H12 closer to each other, which, in turn, repositions H12. The identification of the changed interaction network could provide an explanation for the earlier observed[6,7] differential coregulator binding occurring in phosphorylated PPARγ. The relocation of H12 and H3 displaces the amino acids forming the charged clamp where the coactivators bind [4]. This could explain the loss of binding affinity of coactivator-PPARγ complexes presented in our previous study about coregulator binding to phosphorylated PPARγ [6] . Figure S3 shows the time evolution of the distances in the interaction network of residue 490 averaged over all replicas, emphasizing the dynamics within this interaction network. Again, the preference for higher distances in the network for the WT compared to the PO4 variant is visible.

The bottom part of the ligand binding pocket was previously named “diphenyl pocket”[12], because some partial agonists bind by inserting their diphenyl group deeply into this cavity, which acts as a stabilization pivot between H3, H11, and loop 11/12. In this case, the side chain of residue 310 acts as a gatekeeper of the hydrophobic pocket, being repositioned upon ligand binding. Our CG simulations revealed that residue 310 became less mobile upon S273 phosphorylation by interacting with residues 490 and 491 (Figure 2). This directly affects loops 11/12 and H3, which are involved in PPARγ activation and interaction with coregulators. Variations in this region's hydrophobic packing are believed to impact the dynamics of H12 differently [12].

S273 phosphorylation disturbs the coregulator exchanging PPARγ by changing the dynamics of crucial regions in the receptor

Furthermore, we examined whether S273 phosphorylation affected the protein structure by analyzing the pairwise distance distributions between all BB beads in the PPARγ LBD at CG resolution. Figure 4A displays a matrix with the integrated absolute differences between the distance distributions of WT and PO4 [17]. The resulting values range from 0 to 1.3. To highlight the more noticeable differences, we established a threshold of 0.7 in the upper triangle of the matrix. Figure 4B shows the structure of PPARγ LBD colored by the integrated absolute difference between the BB distance distributions. Residues that exhibit significant structural changes between WT and PO4 are depicted in green, the ones that experienced less structural rearrangements in purple.

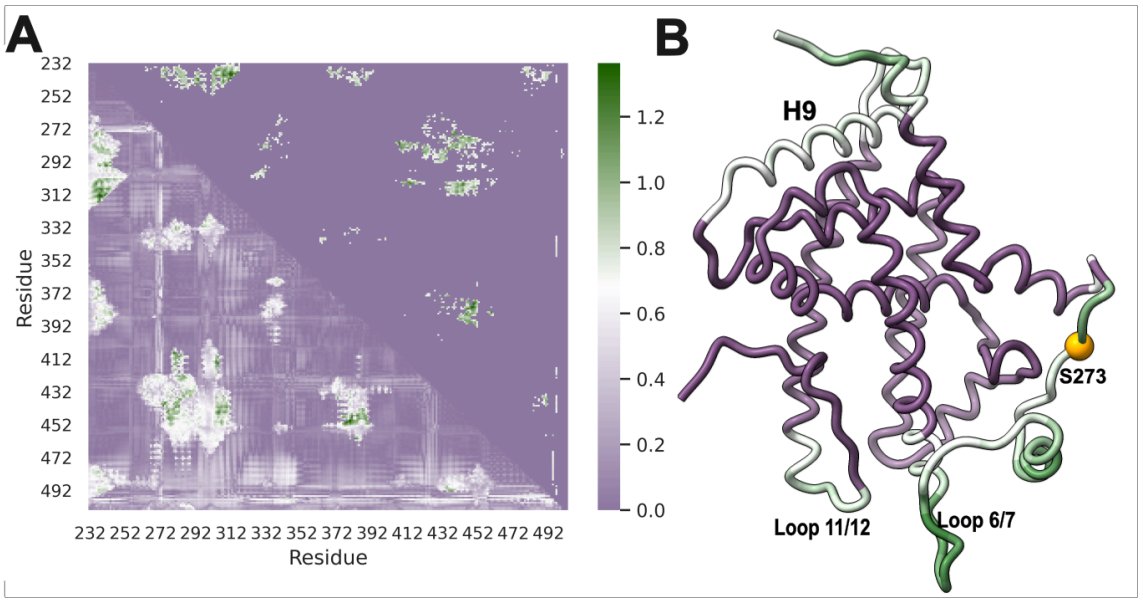

Figure 4 – Structural variation due to S273 phosphorylation during CG simulations. (A) Matrix representation of the integrated absolute difference in distance distributions among all backbone beads of PPARγ LBD. The lower left triangle of the matrix displays the entire dataset variation. The upper triangle shows only values more significant than the threshold (0.7). (B) CG structure of PPARγ LBD colored according to the values of the variance matrix. Residues highlighted in green exhibit an integrated absolute difference exceeding 0.7.

We observed more prominent structural changes in well-known flexible regions such as the loop PO4, loop 6/7, and loop 11/12, which agree well with the RMSD analysis (Figure 1). Moderate differences were also evident in more stable areas, including the entire H9 and specific residues in H1 and H12 (Figure 4B). These findings suggest that S273 phosphorylation affects the structure in the immediate vicinity of the phosphorylation site, as expected, but also impacts residues on the opposite side of the structure, such as residues of H9.

Slight modifications in helixes, such as mutations, can greatly impact the protein structure. The FPLD3-associated L451P mutation in the middle of H9 significantly impairs PPARγ activity. This single-point mutation was sufficient to reduce PPARγ transcriptional activity due to impairment in ligand-mediated coregulator interactions and reduced RXRα heterodimerization and subsequent DNA binding[18]. Another residue in H9 (K450Q) was reported to be a natural mutation in colorectal cancer [19], highlighting the importance of this helix to the proper functioning of PPARγ. Our results show that S273 phosphorylation

increases the RMSD of H9, indicating a gain of flexibility in this region (Figure 1).

Conclusions

We previously demonstrated that S273 phosphorylation leads to modified interaction with different coregulators [6]. The transcription machinery makes precise adjustments to enhance the specificity of each gene. One of these adjustments occurs in the coregulator, which directly interacts with the nuclear receptor. Different coregulators control different genes. Hence, a structural change, such as that presented in this work, could disrupt the coordination of elements in this transcription machinery by altering the primary coregulator that binds to PPARγ.

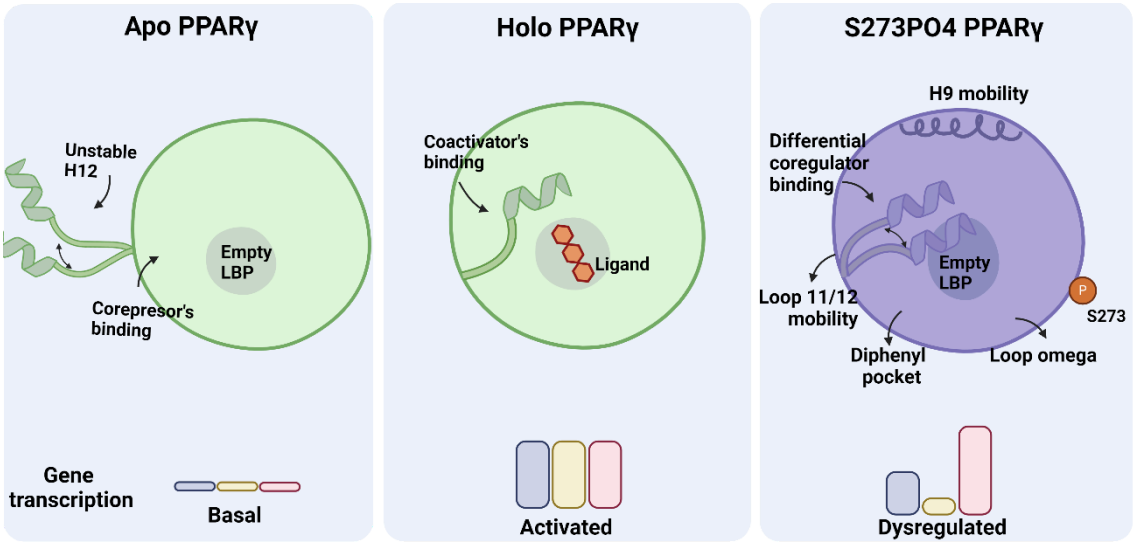

Figure 5 – Suggested PPARγ mechanism of action. Representation of gene regulation by PPARγ in the apo (unbound), holo (bound), and phosphorylated states. Our findings reveal that S273 phosphorylation disrupts the normal functioning of the receptor, potentially inducing altered interactions with corepressors due to structural rearrangements and modifications of dynamics within the receptor at critical regions, namely H9, loop 11/12, diphenyl pocket, and loop 6/7.

The obesity-linked S273 phosphorylation of PPARγ impairs the regular expression of genes related to insulin resistance, mainly by disrupting the

canonical interaction with coregulators. This study demonstrates the potential impact of the S273 phosphorylation as an allosteric regulator that affects the protein's function by changing the protein structure and dynamics of critical regions, particularly of loops 6/7 and 11/12 (Figure 5). This reduces the loops' mobility and affects the diphenyl pocket as well as H12 flexibility. These alterations could modulate the interaction domains of PPARγ with coregulators, as indicated by previous experimental studies [6,7]. Our results indicate that the altered interaction could also result from changes in the mobility of different protein parts, especially of H12, the most important canonical interaction domain, and H9, which is mainly involved in the heterodimerization process, and was previously described as a putative alternative interaction domain with coregulators [18].

Alternative modulation of PPARγ is essential for more effective treatments of obesity-related symptoms and insulin resistance. Notably, our study shows that regions such as the diphenyl pocket, loop 11/12, and H9 have potential as novel target regions for antidiabetic drug candidates to enhance insulin resistance without strongly activating PPARγ. Our results significantly contribute to a better understanding how the transcriptional machinery is fine-tuned in response to metabolic conditions.

Methods

Atomistic simulations

To generate the starting structure, we used the PDB structure 6MS7 [20] containing the LBD of PPARγ. The ligand was removed, and the missing loop (residues 265 to 271 in the γ1 variant) was reconstructed from its amino acid sequence using the CHARMM-GUI PDB Reader & Manipulator program [21] .The same program was used to phosphorylate the S273 residue. All the simulations were carried out for two variants of PPARγ LBD: wild type (WT) and S273 phosphorylated (PO4).

The atomistic simulations were performed using the program package GROMACS (2021.5 version), together with the CHARMM36 force field [22], using

the default parameters setting of CHARMM-GUI. Periodic boundary conditions (PBC) were used, and electrostatic interactions were treated with the Particle-Mesh-Ewald (PME) method. The program automatically determined the grid parameters for the fast Fourier transforms (FFTs). The systems were neutralized and solved in a 0.15 M NaCl solution.

To simulate the protein dynamics, the system was minimized by performing 50 steps of mixed steepest descent (SD) algorithm using the Verlet cut-off scheme. The equilibration was performed using NVT (constant particle number N, volume V, and temperature T) ensemble for 125 ps, with a timestep of Δt=1 fs and followed by a production run with Δt=2 fs for 1 μs in the NPT (constant number of particle N, pressure P, and temperature T) ensemble. During equilibration and production, the temperature was set to T = 303.15 K using a Nose-Hoover thermostat. The Parrinello-Rahman barostat was used with a coupling constant of τ_p=5 ps to maintain 1 bar pressure, which is the default setting by CHARMM-GUI.

Coarse-grained simulations

Equilibrated structures from atomistic simulations were used to generate the CG structures. In this case, the residue S273 (245 in the 6MS7 structure) was mutated into a lysine to provide the proper phosphorylated CG structure. Hence, it was ensured that three beads correspond to the phosphorylated serine when converted into the CG structure. CG simulations used GROMACS (version 2021.5) and the Martini 3 force field [13]. We used the Python package Martinize2/Vermouth[23] for the setup to map the atomistic structure to a CG structure combined with the Gō-like model (GōMartini),[14] with the Leonnard-Jonnes potential of 12 kJ/mol. After generating the CG protein model, the beads corresponding to the phosphorylated S273 were modified to mimic the charge of a phosphorylated serine. Thus, the side chain (SC) beads were replaced by beads of the type TN3a and SD with charge -2.0 in the itp file. The bonded terms were taken from a Martini 2 parametrization of phosphorylated serine [24]. The protein solvation, box neutralization, and addition of a NaCl concentration of 0.15 M were performed with the INSANE script [25].

An initial SD minimization of 2000 steps was performed. This was followed by an equilibration that was carried out in an NPT ensemble employing the v-rescale thermostat to keep the temperature at 300 K. The Berendsen barostat was used with a coupling constant τ_p=5 ps to maintain 1 bar pressure and a timestep of Δt=10 fs for 2.5 ns. Most parameters were kept for the production run except for the barostat, which was set to Parrinello-Rahman, and the coupling constant was increased to τ_p=12 ps. Van der Waals and Coulomb interactions were treated with a cutoff scheme of 1.1 nm. The simulation timestep was increased to Δt=20 fs for a total simulation time of 25 μs. For each PPARγ variant (WT and PO4), 250 μs of simulation (10 replicas of 25 μs each) were conducted.

Analysis of MD simulations

We used the GROMACS tools gmx rmsf and gmx rms and custom Python scripts for root mean square fluctuations (RMSF) and RMSD analyses to analyze the MD simulations. The trajectories were fitted to the rigid BB beads until convergence before any further analysis. The difference RMSD (ΔRMSD) was determined by subtracting PO4 RMSD values from WT RMSD values. We utilized the tool Salt Bridges and Hbonds from Visual Molecular Dynamics (VMD) program package, as well as gmx mindist and gmx distance for residue contact analyses. The GROMACS tool gmx distance was employed to calculate distance distributions between all backbone beads with a bin width of 0.01 nm. To compare the distributions of WT and PO4 PPARγ, we calculated the absolute difference between their backbone bead distributions using the formula described by Souza et al [17]. Where error estimates are given, we employed the block average method, dividing the total simulation time into two blocks to capture long-range transitions while maintaining statistical accuracy. Figures were prepared with Gnuplot, Inkscape, and VMD.

Author contributions

M. M. G. D.: investigation, analysis, writing – original draft, writing – review and editing. C. G. H.: analysis, writing – review and editing. A. C. M. F.:

conceptualization, supervision, writing – review and editing. S. T.: conceptualization, supervision, writing – review and editing.

Conflicts of interest

There are no conflicts to declare.

Data availability

Files to reproduce the simulations in this work are available on Zenodo: 10.5281/zenodo.13264721. Data supporting the findings are available at the corresponding authors upon reasonable request.

Acknowledgments

We acknowledge fruitful discussion with Paulo C. T. Souza. This work was supported by the São Paulo Research Foundation (FAPESP) grants #2019/10274-7 and #2022/05028-0. The authors acknowledge the Frankfurt Institute for Advanced Studies (FIAS) and the Center for Scientific Computing at Goethe University Frankfurt for providing the necessary infrastructure and access to Goethe-HLR. S. T. and C. G. H. thank the Alfons und Gertrud Kassel Foundation, the Dr. Rolf M. Schwiete Foundation, and the Center for Multiscale Modelling in Life Sciences (CMMS) sponsored by the Hessian Ministry of Science and Art for funding. Figure 6 was generated using BioRender.

Notes and References

1. Tontonoz P, Hu E, Spiegelman BM. Stimulation of adipogenesis in fibroblasts by PPARγ2, a lipid-activated transcription factor. Cell. 1994;79(7):1147-1156. doi:10.1016/0092-8674(94)90006-X
2. Lehrke M, Lazar MA. The Many Faces of PPARγ. Cell. 2005;123(6):993-999. doi:10.1016/J.CELL.2005.11.026
3. Guan HP, Ishizuka T, Chui PC, Lehrke M, Lazar MA. Corepressors selectively control the transcriptional activity of PPARγ in adipocytes. Genes Dev. 2005;19(4):453. doi:10.1101/GAD.1263305
4. Savkur RS, Burris TP. The coactivator LXXLL nuclear receptor recognition motif. The Journal of Peptide Research. 2004;63(3):207-212. doi:10.1111/J.1399-3011.2004.00126.X

5. Yu S, Reddy JK. Transcription coactivators for peroxisome proliferator-activated receptors. *Biochim Biophys Acta*. 2007;1771(8):936-951. doi:10.1016/J.BBALIP.2007.01.008
6. Dias MMG, Batista FAH, Tittanegro TH, et al. PPARγ S273 Phosphorylation Modifies the Dynamics of Coregulator Proteins Recruitment. *Front Endocrinol (Lausanne)*. 2020;11(November):1-17. doi:10.3389/fendo.2020.561256
7. Choi JH, Choi SS, Kim ES, et al. Thrap 3 docks on phosphoserine 273 of PPAR γ and controls diabetic gene programming. *Genes Dev*. 2018;28:2361-2369. doi:10.1101/gad.249367.114
8. Choi JH, Banks AS, Estall JL, et al. Anti-diabetic drugs inhibit obesity-linked phosphorylation of PPARγ by Cdk5. *Nature*. 2010;466(7305):451-456. doi:10.1038/nature09291
9. Choi JH, Banks AS, Kamenecka TM, et al. Antidiabetic actions of a non-agonist PPARγ ligand blocking Cdk5-mediated phosphorylation. *Nature*. 2011;477(7365):477-481. doi:10.1038/nature10383
10. Choi SS, Kim ES, Jung JE, et al. PPARg antagonist gleevec improves insulin sensitivity and promotes the browning of white adipose tissue. *Diabetes*. 2016;65(4):829-839. doi:10.2337/db15-1382
11. Choi SS, Kim ES, Koh M, et al. A novel non-agonist peroxisome proliferator-activated receptor γ (PPARγ) ligand UHC1 blocks PPARγ phosphorylation by cyclin-dependent kinase 5 (CDK5) and improves insulin sensitivity. *Journal of Biological Chemistry*. 2014;289(38):26618-26629. doi:10.1074/jbc.M114.566794
12. Montanari R, Saccoccia F, Scotti E, et al. Crystal structure of the peroxisome proliferator-activated receptor γ (PPARγ) ligand binding domain complexed with a novel partial agonist: A new region of the hydrophobic pocket could be exploited for drug design. *J Med Chem*. 2008;51(24):7768-7776. doi:10.1021/jm800733h
13. Souza PCT, Alessandri R, Barnoud J, et al. Martini 3: a general purpose force field for coarse-grained molecular dynamics. *Nature Methods 2021 18:4*. 2021;18(4):382-388. doi:10.1038/s41592-021-01098-3
14. Souza PCT, Borges-Araújo L, Brasnett C, et al. GōMartini 3: From large conformational changes in proteins to environmental bias corrections. *bioRxiv*. Published online April 16, 2024:2024.04.15.589479. doi:10.1101/2024.04.15.589479
15. Hegele RA, Cao H, Frankowski C, Mathews ST, Leff T. *Brief Genetics Report PPARG F388L, a Transactivation-Deficient Mutant, in Familial Partial Lipodystrophy*. http://diabetesjournals.org/diabetes/article-pdf/51/12/3586/652871/db1202003586.pdf
16. Lori C, Pasquo A, Montanari R, et al. Structural basis of the transactivation deficiency of the human PPARγ F360L mutant associated

with familial partial lipodystrophy. *Acta Crystallogr D Biol Crystallogr*. 2014;70(7):1965-1976. doi:10.1107/S1399004714009638

17. Souza PCT, Thallmair S, Marrink SJ, Mera-Adasme R. An Allosteric Pathway in Copper, Zinc Superoxide Dismutase Unravels the Molecular Mechanism of the G93A Amyotrophic Lateral Sclerosis-Linked Mutation. *Journal of Physical Chemistry Letters*. 2019;10(24):7740-7744. doi:10.1021/acs.jpclett.9b02868
18. Broekema MF, Massink MPG, Donato C, et al. Natural helix 9 mutants of PPARγ differently affect its transcriptional activity. *Mol Metab*. 2019;20:115-127. doi:10.1016/j.molmet.2018.12.005
19. Gupta RA, Sarraf P, Mueller E, et al. Peroxisome Proliferator-activated Receptor γ-mediated Differentiation. *Journal of Biological Chemistry*. 2003;278(25):22669-22677. doi:10.1074/jbc.m300637200
20. Jiang H, Zhou XE, Shi J, et al. Identification and structural insight of an effective PPARγ modulator with improved therapeutic index for anti-diabetic drug discovery. *Chem Sci*. 2020;11(8):2260-2268. doi:10.1039/C9SC05487A
21. Jo S, Kim T, Iyer VG, Im W. CHARMM-GUI: A web-based graphical user interface for CHARMM. *J Comput Chem*. 2008;29(11):1859-1865. doi:10.1002/JCC.20945
22. Vanommeslaeghe K, Hatcher E, Acharya C, et al. CHARMM general force field: A force field for drug-like molecules compatible with the CHARMM all-atom additive biological force fields. *J Comput Chem*. 2010;31(4):671-690. doi:10.1002/JCC.21367
23. Kroon PC, Grunewald F, Barnoud J, et al. Martinize2 and Vermouth: Unified Framework for Topology Generation. *Elife*. 2023;12. doi:10.7554/ELIFE.90627
24. Pluhackova K, Wilhelm FM, Müller DJ. Lipids and Phosphorylation Conjointly Modulate Complex Formation of β2-Adrenergic Receptor and β-arrestin2. *Front Cell Dev Biol*. 2021;9:807913. doi:10.3389/FCELL.2021.807913/BIBTEX
25. Wassenaar TA, Ingólfsson HI, Böckmann RA, Tieleman DP, Marrink SJ. Computational lipidomics with insane: A versatile tool for generating custom membranes for molecular simulations. *J Chem Theory Comput*. 2015;11(5):2144-2155. doi:10.1021/ACS.JCTC.5B00209/SUPPL_FILE/CT5B00209_SI_001.PDF

4. DISCUSSÃO

Esse estudo explorou os achados de dois artigos que abordaram os diferentes aspectos das consequências da fosforilação da S273, fornecendo um entendimento abrangente sobre a significância biológica desse PTM.

Nosso primeiro artigo investiga como a fosforilação do S273 altera a interação entre o PPARγ e várias proteínas coreguladoras. Ele revela que essa fosforilação altera o equilíbrio entre coativadores e corepressores, levando a alteração do perfil de expressão de genes relacionados à adipogênese e à sensibilidade à insulina, descritos anteriormente [34,43]. Foi visto que quando o S273 é fosforilada, o PPARγ apresenta uma interação reduzida com corepressor como o NCoR ao mesmo tempo que aumenta a interação com coativadores como PGC1-α e TIF2. Essa alteração afeta também as preferências de domínios de inteiração (IDs) pelos quais os coreguladores se ligam ao PPARγ. Essa mudança na dinâmica de interação sugere que a fosforilação S273 pode servir como um interruptor molecular, modulando a atividade transcricional do PPARγ em resposta a sinais metabólicos.

A compreensão de como a fosforilação da S273 altera o perfil de interação PPARγ-corregulador fornece informações sobre os mecanismos da resistência à insulina induzida pela obesidade. A manutenção das interações apropriadas para cada corregulador é importante para preservar as funções metabólicas benéficas do PPARγ.

Atualmente, as estratégias que modulam o estado de fosforilação de S273 são majoritariamente dependentes de ligantes [34,43,44], para isso desenvolveram-se novos ligantes que são capazes de se ligar e bloquear a fosforilação com pouca ou nenhuma alteração do perfil de ativação do PPARγ. Com o esclarecimento das mudanças no equilíbrio da troca dos coreguladores é possível pensar em novas estratégias que tenham como alvo direto as interfaces de interação dos coreguladores como oportunidades terapêuticas para doenças metabólicas. Ao restaurar o equilíbrio das interações do coativador e do corepressor, pode ser possível normalizar a atividade do PPARγ e melhorar os resultados metabólicos.

No segundo artigo, nós buscamos uma compreensão mais profunda do mecanismo estrutural que levaria a interação diferencial com os coreguladores. Para isso, nós exploramos se a fosforilação poderia alterar os movimentos e interações intramoleculares necessários para o funcionamento normal do PPARy. Nós obtivemos evidências de que essa fosforilação afeta o recrutamento de coreguladores por meio de alterações o estado conformacional do receptor, afetando sua função geral.

Através de dinâmicas moleculares nós observamos que fosforilação de S273 leva a alterações notáveis da estrutura e da dinâmica de regiões críticas da proteína, principalmente dos loops 6/7 e 11/12. Isso reduz a mobilidade dos loops e afeta uma região chamada de “diphenyl pocket” que compreende a H3, loop11/12 e loop 6/7, e consequentemente altera a flexibilidade do H12, região canônica de interação com os coreguladores. Além disso, nós também observamos uma mudança na estabilidade da H9, região descrita anteriormente como um domínio de interação alternativo com os coreguladores.

Como a maquinaria de transcrição depende de ajustes finos para aumentar a especificidade de cada gene, mudanças de flexibilidade como as observadas por nós poderia afetar diretamente a interação com o corregulador primário, que interage diretamente com o receptor nuclear, o que levaria a um ajuste de toda a maquinaria de transcrição subsequente. O que por sua vez pode afetar todo o perfil de expressão gênica.

5. CONCLUSÃO

Em conjunto, esses dois estudos elucidam a função complexa da fosforilação S273 do PPARγ na regulação da função do receptor. A capacidade da fosforilação S273 de modular as interações com coreguladores, alterar a dinâmica do receptor e interagir com outras modificações pós-traducionais destaca sua importância na regulação metabólica. Dada a associação da desregulação do PPARγ com condições como obesidade e resistência à insulina, a compreensão desses mecanismos pode abrir caminho para novas estratégias terapêuticas direcionadas ao PPARγ. Esses achados apresentam alternativas para a modulação das vias moleculares precisas envolvidas e no status de fosforilação da S273 do PPARγ para melhorar a saúde metabólica. Em conclusão, a integração das descobertas desses dois artigos fornece uma visão geral abrangente de como a fosforilação S273 do PPARγ atua como um nó regulador crítico na intrincada rede de sinalização metabólica, enfatizando seu potencial como alvo terapêutico em distúrbios metabólicos.

6. REFERÊNCIAS

1. Chooi YC, Ding C, Magkos F. The epidemiology of obesity. Metabolism. 2019;92:6-10. doi:10.1016/J.METABOL.2018.09.005

2. Muir LA, Neeley CK, Meyer KA, et al. Adipose tissue fibrosis, hypertrophy, and hyperplasia: Correlations with diabetes in human obesity. Obesity. 2016;24(3):597-605. doi:10.1002/OBY.21377

3. di Bonito P, Valerio G, Licenziati MR, et al. Uric acid, impaired fasting glucose and impaired glucose tolerance in youth with overweight and obesity. Nutrition, Metabolism and Cardiovascular Diseases. 2021;31(2):675-680. doi:10.1016/J.NUMECD.2020.10.007

4. Nieto-Vazquez I, Fernández-Veledo S, Krämer DK, Vila-Bedmar R, Garcia-Guerra L, Lorenzo M. Insulin resistance associated to obesity: the link TNF-alpha. https://doi.org/101080/13813450802181047. 2008;114(3):183-194. doi:10.1080/13813450802181047

5. Group PL, Sell (H, Eckel J, Sell H, Habich C, Eckel J. Adaptive immunity in obesity and insulin resistance. Nature Reviews Endocrinology 2012 8:12. 2012;8(12):709-716. doi:10.1038/nrendo.2012.114

6. Nishimura S, Manabe I, Nagasaki M, et al. CD8+ effector T cells contribute to macrophage recruitment and adipose tissue inflammation in obesity. Nature Medicine 2009 15:8. 2009;15(8):914-920. doi:10.1038/nm.1964

7. Arkan MC, Hevener AL, Greten FR, et al. IKK-β links inflammation to obesity-induced insulin resistance. Nature Medicine 2005 11:2. 2005;11(2):191-198. doi:10.1038/nm1185

8. Hirosumi J, Tuncman G, Chang L, et al. A central role for JNK in obesity and insulin resistance. Nature 2002 420:6913. 2002;420(6913):333-336. doi:10.1038/nature01137

9. Tanti JF, Ceppo F, Jager J, Berthou F. Implication of inflammatory signaling pathways in obesity-induced insulin resistance. Front Endocrinol (Lausanne). 2013;3(JAN):181. doi:10.3389/FENDO.2012.00181/BIBTEX

10. Christian Weyer TFSTKHYMREPPAT. Hypoadiponectinemia in Obesity and Type 2 Diabetes: Close Association with Insulin Resistance and Hyperinsulinemia. Clinical Diabetes and Nutrition Section. Published online 2001. Accessed March 28, 2022. https://academic.oup.com/jcem/article/86/5/1930/2848024

11. Nanjan MJ, Mohammed M, Prashantha Kumar BR, Chandrasekar MJN. Thiazolidinediones as antidiabetic agents: A critical review. Bioorg Chem. 2018;77:548-567. doi:10.1016/J.BIOORG.2018.02.009

12. Tontonoz P, Spiegelman BM. Fat and Beyond: The Diverse Biology of PPARγ. https://doi.org/101146/annurev.biochem77061307091829. 2008;77:289-312. doi:10.1146/ANNUREV.BIOCHEM.77.061307.091829

13. Ceriello A. Thiazolidinediones as anti-inflammatory and anti-atherogenic agents. Diabetes Metab Res Rev. 2008;24(1):14-26. doi:10.1002/DMRR.790

14. Berlie HD, Kalus JS, Jaber LA. Thiazolidinediones and the risk of edema: A meta-analysis. Diabetes Res Clin Pract. 2007;76(2):279-289. doi:10.1016/J.DIABRES.2006.09.010

15. Billington EO, Grey A, Bolland MJ. The effect of thiazolidinediones on bone mineral density and bone turnover: systematic review and meta-analysis. Diabetologia. 2015;58(10):2238-2246. doi:10.1007/S00125-015-3660-2/FIGURES/3

16. Lago RM, Singh PP, Nesto RW. Congestive heart failure and cardiovascular death in patients with prediabetes and type 2 diabetes given thiazolidinediones: a meta-analysis of randomised clinical trials. The Lancet. 2007;370(9593):1129-1136. doi:10.1016/S0140-6736(07)61514-1

17. Antonietta Ajmone-Cat M, Lavinia Salvatori M, de Simone R, et al. Docosahexaenoic acid modulates inflammatory and antineurogenic functions of activated microglial cells. J Neurosci Res. 2012;90(3):575-587. doi:10.1002/JNR.22783

18. Marion-Letellier R, Savoye G, Ghosh S. Fatty acids, eicosanoids and PPAR gamma. Eur J Pharmacol. 2016;785:44-49. doi:10.1016/J.EJPHAR.2015.11.004

19. Sun K, Kusminski CM, Scherer PE. Adipose tissue remodeling and obesity. J Clin Invest. 2011;121(6):2094-2101. doi:10.1172/JCI45887

20. Zhang Y, Proenca R, Maffei M, Barone M, Leopold L, Friedman JM. Positional cloning of the mouse obese gene and its human homologue. Nature 1994 372:6505. 1994;372(6505):425-432. doi:10.1038/372425a0

21. Rutkowski JM, Stern JH, Scherer PE. The cell biology of fat expansion. Journal of Cell Biology. 2015;208(5):501-512. doi:10.1083/JCB.201409063

22. Lo JC, Ljubicic S, Leibiger B, et al. Adipsin is an adipokine that improves β cell function in diabetes. Cell. 2014;158(1):41-53. doi:10.1016/J.CELL.2014.06.005

23. Guan HP, Ishizuka T, Chui PC, Lehrke M, Lazar MA. Corepressors selectively control the transcriptional activity of PPARgamma in adipocytes. Genes Dev. 2005;19(4):453-461. doi:10.1101/GAD.1263305

24. Savkur RS, Burris TP. The coactivator LXXLL nuclear receptor recognition motif. The Journal of Peptide Research. 2004;63(3):207-212. doi:10.1111/J.1399-3011.2004.00126.X

25. Yu S, Reddy JK. Transcription coactivators for peroxisome proliferator-activated receptors. Biochim Biophys Acta. 2007;1771(8):936-951. doi:10.1016/J.BBALIP.2007.01.008

26. Brunmeir R, Xu F. Functional Regulation of PPARs through Post-Translational Modifications. International Journal of Molecular Sciences 2018, Vol 19, Page 1738. 2018;19(6):1738. doi:10.3390/IJMS19061738

27. Choi JH, Banks AS, Estall JL, et al. Anti-diabetic drugs inhibit obesity-linked phosphorylation of PPARγ by Cdk5. Nature 2010 466:7305. 2010;466(7305):451-456. doi:10.1038/nature09291

28. Qiang L, Wang L, Kon N, et al. Brown remodeling of white adipose tissue by SirT1-dependent deacetylation of Pparγ. Cell. 2012;150(3):620-632. doi:10.1016/J.CELL.2012.06.027/ATTACHMENT/C597E177-2C9A-4B16-B13B-F07DD3FBF85F/MMC1.PDF

29. Choi JH, Banks AS, Kamenecka TM, et al. Antidiabetic actions of a non-agonist PPARγ ligand blocking Cdk5-mediated phosphorylation. Nature 2011 477:7365. 2011;477(7365):477-481. doi:10.1038/nature10383

30. Choi S, Jung JE, Yang YR, et al. Novel phosphorylation of PPARγ ameliorates obesity-induced adipose tissue inflammation and improves insulin sensitivity. Cell Signal. 2015;27(12):2488-2495. doi:10.1016/J.CELLSIG.2015.09.009

31. Filho HVR, Videira NB, Bridi AV, et al. Screening for PPAR non-agonist ligands followed by characterization of a hit, AM-879, with additional no-adipogenic and cdk5-mediated phosphorylation inhibition properties. Front Endocrinol (Lausanne). 2018;9(FEB):11. doi:10.3389/FENDO.2018.00011/BIBTEX

32. Choi SS, Kim ES, Koh M, et al. A novel non-agonist peroxisome proliferator-activated receptor γ (PPARγ) ligand UHC1 blocks PPARγ phosphorylation by cyclin-dependent kinase 5 (CDK5) and improves insulin sensitivity. J Biol Chem. 2014;289(38):26618-26629. doi:10.1074/JBC.M114.566794

33. Amato AA, Rajagopalan S, Lin JZ, et al. GQ-16, a novel peroxisome proliferator-activated receptor γ (PPARγ) ligand, promotes insulin sensitization without weight gain. Journal of Biological Chemistry. 2012;287(33):28169-28179. doi:10.1074/JBC.M111.332106/ATTACHMENT/B6448337-EC8A-4473-8536-F6FA30ED6219/MMC1.PDF

34. Hermanson O, Glass CK, Rosenfeld MG. Nuclear receptor coregulators: multiple modes of modification. Trends Endocrinol Metab. 2002;13(2):55-60. doi:10.1016/S1043-2760(01)00527-6

35. Choi JH, Choi SS, Kim ES, et al. Thrap 3 docks on phosphoserine 273 of PPAR γ and controls diabetic gene programming. Genes Dev. 2018;28:2361-2369. doi:10.1101/gad.249367.114

36. Zanoni I, Ostuni R, Marek LR, et al. CD14 Controls the LPS-Induced Endocytosis of Toll-like Receptor 4. Cell. 2011;147(4):868-880. doi:10.1016/J.CELL.2011.09.051

37. Dias MMG, Batista FAH, Tittanegro TH, et al. PPARγ S273 Phosphorylation Modifies the Dynamics of Coregulator Proteins Recruitment. Front Endocrinol (Lausanne). 2020;11(November):1-17. doi:10.3389/fendo.2020.561256

38. Puigserver P, Wu Z, Park CW, Graves R, Wright M, Spiegelman BM. A cold-inducible coactivator of nuclear receptors linked to adaptive thermogenesis. Cell. 1998;92(6):829-839. doi:10.1016/S0092-8674(00)81410-5

39. Liang H, Ward WF. PGC-1α: A key regulator of energy metabolism. American Journal of Physiology - Advances in Physiology Education. 2006;30(4):145-151. doi:10.1152/ADVAN.00052.2006/ASSET/IMAGES/LARGE/ZU10040623260001.JPEG

40. Ravussin E, Galgani JE. The Implication of Brown Adipose Tissue for Humans. http://dx.doi.org/101146/annurev-nutr-072610-145209. 2011;31:33-47. doi:10.1146/ANNUREV-NUTR-072610-145209

41. Hibi M, Oishi S, Matsushita M, et al. Brown adipose tissue is involved in diet-induced thermogenesis and whole-body fat utilization in healthy humans. International Journal of Obesity 2016 40:11. 2016;40(11):1655-1661. doi:10.1038/ijo.2016.124

42. Farmer SR. Be cool, lose weight. Nature 2009 458:7240. 2009;458(7240):839-840. doi:10.1038/458839a

43. Virtanen KA, Nuutila P. Brown adipose tissue in humans. Curr Opin Lipidol. 2011;22(1). doi:10.1097/MOL.0B013E3283425243

44. Liu L, Fan L, Chan M, et al. PPARγ Deacetylation Confers the Antiatherogenic Effect and Improves Endothelial Function in Diabetes Treatment. Diabetes. 2020;69(8):1793-1803. doi:10.2337/DB20-0217

45. Seale P, Conroe HM, Estall J, et al. Prdm16 determines the thermogenic program of subcutaneous white adipose tissue in mice. J Clin Invest. 2011;121(1):96-105. doi:10.1172/JCI44271

46. Boyes J, Byfield P, Nakatani Y, Ogryzko V. Regulation of activity of the transcription factor GATA-1 by acetylation. Nature 1998 396:6711. 1998;396(6711):594-598. doi:10.1038/25166

47. Imhof A, Yang XJ, Ogryzko V v., Nakatani Y, Wolffe AP, Ge H. Acetylation of general transcription factors by histone acetyltransferases. Current Biology. 1997;7(9):689-692. doi:10.1016/S0960-9822(06)00296-X

48. Chen H, Lin RJ, Xie W, Wilpitz D, Evans RM. Regulation of Hormone-Induced Histone Hyperacetylation and Gene Activation via Acetylation of an Acetylase. Cell. 1999;98(5):675-686. doi:10.1016/S0092-8674(00)80054-9

49. Picard F, Kurtev M, Chung N, et al. Sirt1 promotes fat mobilization in white adipocytes by repressing PPAR-γ. Nature 2004 429:6993. 2004;429(6993):771-776. doi:10.1038/nature02583

50. Lowell BB, Spiegelman BM. Towards a molecular understanding of adaptive thermogenesis. Nature 2000 404:6778. 2000;404(6778):652-660. doi:10.1038/35007527

51. Wu Z, Puigserver P, Andersson U, et al. Mechanisms Controlling Mitochondrial Biogenesis and Respiration through the Thermogenic Coactivator PGC-1. Cell. 1999;98(1):115-124. doi:10.1016/S0092-8674(00)80611-X

52. Choi JH, Banks AS, Estall JL, et al. Anti-diabetic drugs inhibit obesity-linked phosphorylation of PPARγ by Cdk5. Nature. 2010;466(7305):451-456. doi:10.1038/nature09291

53. Choi JH, Banks AS, Kamenecka TM, et al. Antidiabetic actions of a non-agonist PPARγ ligand blocking Cdk5-mediated phosphorylation. Nature. 2011;477(7365):477-481. doi:10.1038/nature10383

54. Choi SS, Kim ES, Jung JE, et al. PPARg antagonist gleevec improves insulin sensitivity and promotes the browning of white adipose tissue. Diabetes. 2016;65(4):829-839. doi:10.2337/db15-1382

55. Mottin M, Souza PCT, Skaf MS. Molecular Recognition of PPARγ by Kinase Cdk5/p25: Insights from a Combination of Protein-Protein Docking and Adaptive Biasing Force Simulations. Journal of Physical Chemistry B. 2015;119(26):8330-8339. doi:10.1021/acs.jpcb.5b04269

56. Ribeiro Filho HV, Guerra JV, Cagliari R, et al. Exploring the mechanism of PPARγ phosphorylation mediated by CDK5. J Struct Biol. 2019;207(3):317-326. doi:10.1016/j.jsb.2019.07.007

57. He Y, B'nai Taub A, Yu L, et al. PPARγ Acetylation Orchestrates Adipose Plasticity and Metabolic Rhythms. Advanced Science. 2023;10(2):2204190. doi:10.1002/ADVS.202204190

58. Terra MF, García-Arévalo M, Avelino TM, et al. Obesity-Linked PPARγ Ser273 Phosphorylation Promotes Beneficial Effects on the Liver, despite Reduced Insulin Sensitivity in Mice. Biomolecules. 2023;13(4):632. doi:10.3390/BIOM13040632/S1

7. APÊNDICES

7.1. APÊNDICE A - Artigo com primeira autoria compartilhada: Multifactorial Basis and Therapeutic Strategies in Metabolism-Related Diseases

Review

Multifactorial Basis and Therapeutic Strategies in Metabolism-Related Diseases

João V. S. Guerra [1,2,†], Marieli M. G. Dias [1,3,†], Anna J. V. C. Brilhante [3,4], Maiara F. Terra [1,3], Marta García-Arévalo [1,*] and Ana Carolina M. Figueira [1,*]

1 Brazilian Center for Research in Energy and Materials (CNPEM), Brazilian Biosciences National Laboratory (LNBio), Polo II de Alta Tecnologia—R. Giuseppe Máximo Scolfaro, Campinas 13083-100, Brazil; joao.guerra@lnbio.cnpem.br (J.V.S.G.); marieli.dias@lnbio.cnpem.br (M.M.G.D.); maiara.terra@lnbio.cnpem.br (M.F.T.)
2 Graduate Program in Pharmaceutical Sciences, Faculty Pharmaceutical Sciences, University of Campinas, Campinas 13083-970, Brazil
3 Graduate Program in Functional and Molecular Biology, Institute of Biology, State University of Campinas (Unicamp), Campinas 13083-970, Brazil; anna.brilhante@lnbr.cnpem.br
4 Brazilian Center for Research in Energy and Materials (CNPEM), Brazilian Biorenewables National Laboratory (LNBR), Polo II de Alta Tecnologia—R. Giuseppe Máximo Scolfaro, Campinas 13083-100, Brazil
* Correspondence: marta.provencio@lnbio.cnem.br or mgarciaarevalo@hotmail.com (M.G.-A.); ana.figueira@lnbio.cnpem.br (A.C.M.F.)
† Both authors contributed equally to this work.

Abstract: Throughout the 20th and 21st centuries, the incidence of non-communicable diseases (NCDs), also known as chronic diseases, has been increasing worldwide. Changes in dietary and physical activity patterns, along with genetic conditions, are the main factors that modulate the metabolism of individuals, leading to the development of NCDs. Obesity, diabetes, metabolic associated fatty liver disease (MAFLD), and cardiovascular diseases (CVDs) are classified in this group of chronic diseases. Therefore, understanding the underlying molecular mechanisms of these diseases leads us to develop more accurate and effective treatments to reduce or mitigate their prevalence in the population. Given the global relevance of NCDs and ongoing research progress, this article reviews the current understanding about NCDs and their related risk factors, with a focus on obesity, diabetes, MAFLD, and CVDs, summarizing the knowledge about their pathophysiology and highlighting the currently available and emerging therapeutic strategies, especially pharmacological interventions. All of these diseases play an important role in the contamination by the SARS-CoV-2 virus, as well as in the progression and severity of the symptoms of the coronavirus disease 2019 (COVID-19). Therefore, we briefly explore the relationship between NCDs and COVID-19.

Keywords: NCDs; obesity; diabetes; MAFLD; cardiovascular diseases; metabolism

Citation: Guerra, J.V.S.; Dias, M.M.G.; Brilhante, A.J.V.C.; Terra, M.F.; García-Arévalo, M.; Figueira, A.C.M. Multifactorial Basis and Therapeutic Strategies in Metabolism-Related Diseases. *Nutrients* **2021**, *13*, 2830. https://doi.org/10.3390/nu13082830

Academic Editor: Sebastiano Banni

Received: 28 June 2021
Accepted: 11 August 2021
Published: 18 August 2021

7.2. *APÊNDICE B- Artigo publicado em colaboração: pH and the Breast Cancer Recurrent Mutation D538G Affect the Process of Activation of Estrogen Receptor α*

Biochemistry

pubs.acs.org/biochemistry Article

pH and the Breast Cancer Recurrent Mutation D538G Affect the Process of Activation of Estrogen Receptor α

Vinícius M. de Oliveira, Marieli M. G. Dias, Thayná M. Avelino, Natália B. Videira, Fernando B. da Silva, Tábata R. Doratioto, Paul C. Whitford, Vitor B. P. Leite,* and Ana Carolina M. Figueira*

Cite This: *Biochemistry* 2022, 61, 455−463 Read Online

ACCESS | Metrics & More | Article Recommendations | Supporting Information

ABSTRACT: Estrogen receptor α (ERα) is a regulatory protein that can access a set of distinct structural configurations. ERα undergoes extensive remodeling as it interacts with different agonists and antagonists, as well as transcription activation and repression factors. Moreover, breast cancer tumors resistant to hormone therapy have been associated with the imbalance between the active and inactive ERα states. Cancer-activating mutations in ERα play a crucial role in this imbalance and can promote the progression of cancer. However, the rate of this progression can also be increased by dysregulated pH in the tumor microenvironment. Many molecular aspects of the process of activation of ERα that can be affected by these pH changes and mutations are still unclear. Thus, we applied computational and experimental techniques to explore the activation process dynamics of ER for environments with different pHs and in the presence of one of the most recurrent cancer-activating mutations, D538G. Our results indicated that the effect of the pH increase associated with the D538G mutation promoted a robust stabilization of the active state of ER. We were also able to determine the main protein regions that have the most potential to influence the activation process under different pH conditions, which may provide targets of future therapeutics for the treatment of hormone-resistant breast cancer tumors. Finally, the approach used here can be applied for proteins associated with the proliferation of other cancer types, which can also have their function affected by small pH changes.

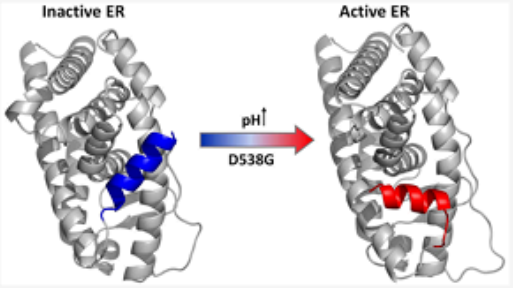

7.3. APÊNDICE C – Artigo em publicado em colaboraçao: Mass spectrometry-based proteomics of 3D cell culture: A useful tool to validate culture of spheroids and organoids

ARTICLE IN PRESS

JID: SLASD [m5GeSdc;November 9, 2021;14:57]

SLAS Discovery xxx (xxxx) xxx

Contents lists available at ScienceDirect

SLAS Discovery

journal homepage: www.elsevier.com/locate/slasd

Full Length Article

Mass spectrometry-based proteomics of 3D cell culture: A useful tool to validate culture of spheroids and organoids

Thayna Mendonca Avelino[a,b], Marta García-Arévalo[a], Felipe Rafael Torres[a], Marieli Mariano Goncalves Dias[a,c], Romenia Ramos Domingues[a], Murilo de Carvalho[a], Matheus de Castro Fonseca[a], Vanessa Kiraly Thomaz Rodrigues[a], Adriana Franco Paes Leme[a], Ana Carolina Migliorini Figueira[a,b,c,*]

[a] National Center of Research in Energy and Materials (CNPEM), National Laboratory of Bioscience (LNBio)
[b] State University of Campinas (UNICAMP), Department of Pharmacology Science
[c] State University of Campinas (UNICAMP), Department of Molecular and Functional Biology

ARTICLE INFO

Keywords:
Spheroids
Obesity
Adipogenesis
Mass spectrometry
Proteomics

ABSTRACT

Worldwide obesity, defined as abnormal or excessive fat accumulation that may result in different comorbidities, is considered a pandemic condition that has nearly tripled in the last 45 years. Most studies on obesity use animal models or adipocyte monolayer cell culture to investigate adipose tissue. However, besides monolayer cell culture approaches do not fully recapitulate the physiology of living organisms, there is a growing need to reduce or replace animals in research. In this context, the development of 3D self-organized structures has provided models that better reproduce the in vitro aspects of the in vivo physiology in comparison to traditional monolayer cell culture.

Besides, recent advances in omics technologies have allowed us to characterize these cultures at the proteome, metabolome, transcription factor, DNA-binding and transcriptomic levels. These two combined approaches, 3D culture and omics, have provided more realistic data about determined conditions. Thereby, here we focused on the development of an obesity study pipeline including proteomic analysis to validate adipocyte-derived spheroids. Through the combination of collected mass spectrometry data from differentiated 3T3-L1 spheroids and from murine white adipose tissue (WAT), we identified 1732 proteins in both samples. By using a comprehensive proteomic analysis, we observed that the in vitro 3D culture of differentiated adipocytes shares important molecular pathways with the WAT, including expression of proteins involved in central metabolic process of the adipose tissue. Together, our results show a combination of an orthogonal method and an image-based analysis that constitutes a useful pipeline to be applied in 3D adipocyte culture.

7.4. APÊNDICE D – Artigo publicado em colaboração: SARS-CoV-2 uses CD4 to infect T helper lymphocytes

Research Article

Immunology and Inflammation

SARS-CoV-2 uses CD4 to infect T helper lymphocytes

Natalia S Brunetti, Gustavo G Davanzo, Diogo de Moraes, Allan JR Ferrari, Gabriela F Souza, Stéfanie Primon Muraro, Thiago L Knittel, Vinicius O Boldrini, Lauar B Monteiro, João Victor Virgílio-da-Silva, Gerson S Profeta, Natália S Wassano, Luana Nunes Santos, Victor C Carregari, Artur HS Dias, Flavio P Veras, Lucas A Tavares, Julia Forato, Icaro MS Castro, Lícia C Silva-Costa, André C Palma, Eli Mansour, Raisa G Ulaf, Ana F Bernardes, Thyago A Nunes, Luciana C Ribeiro, Marcus V Agrela, Maria Luiza Moretti, Lucas I Buscaratti, Fernanda Crunfli, Raissa G Ludwig, Jaqueline A Gerhardt, Natália Munhoz-Alves, Ana Maria Marques, Renata Sesti-Costa, Mariene R Amorim, Daniel A Toledo-Teixeira, Pierina Lorencini Parise, Matheus Cavalheiro Martini, Karina Bispos-dos-Santos, Camila L Simeoni, Fabiana Granja, Virgínia C Silvestrini, Eduardo B de Oliveira, Vitor M Faca, Murilo Carvalho, Bianca G Castelucci, Alexandre B Pereira, Laís D Coimbra, Marieli MG Dias, Patricia B Rodrigues, Arilson Bernardo SP Gomes, Fabricio B Pereira, Leonilda MB Santos, Louis-Marie Bloyet, Spencer Stumpf, Marjorie C Pontelli, Sean Whelan, Andrei C Sposito, Robson F Carvalho, André S Vieira, Marco AR Vinolo, André Damasio, Licio Velloso, Ana Carolina M Figueira, Luis LP da Silva, Thiago Mattar Cunha, Helder I Nakaya, Henrique Marques-Souza, Rafael E Marques, Daniel Martins-de-Souza, Munir S Skaf, Jose Luiz Proenca-Modena, Pedro MM Moraes-Vieira, Marcelo A Mori, Alessandro S Farias « see less

Autoimmune Research Laboratory, Department of Genetics, Microbiology and Immunology, Institute of Biology, University of Campinas (UNICAMP), Brazil; Laboratory of Immunometabolism, Department of Genetics, Microbiology and Immunology, Institute of Biology, University of Campinas (UNICAMP), Brazil; Laboratory of Aging Biology, Department of Biochemistry and Tissue Biology, Institute of Biology, University of Campinas (UNICAMP), Brazil; Department of Structural and Functional Biology, Institute of Biosciences, Sao Paulo State University (UNESP), Brazil; Institute of Chemistry and Center for Computing in

7.5. APÊNDICE E – Capítulo de livro: PPAR Modulation Through Posttranslational Modification Control

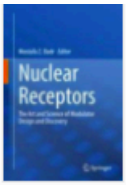

Nuclear Receptors pp 537-611 | Cite as

PPAR Modulation Through Posttranslational Modification Control

Authors | Authors and affiliations

Natália B. Videira, Marieli M. G. Dias, Maiara F. Terra, Vinicius M. de Oliveira, Marta García-Arévalo, Thayná M. Avelino, Felipe R. Torres, Fernanda A. H. Batista, Ana Carolina M. Figueira

Chapter
First Online: 29 September 2021

Abstract

The peroxisome proliferator-activated receptors (PPAR) are transcription factors modulated by ligands and members of the nuclear receptor superfamily. There are three different human PPAR isotypes: PPARα, PPARδ/β, and PPARγ, which regulate the transcription of their target genes involved with energy metabolism, inflammatory process, and cellular differentiation in different human tissues. Because of these activities, PPARs are considered important targets for drugs to treat metabolic diseases, including diabetes, dyslipidemia, and obesity. Besides ligand modulation, PPARs activities can be modulated by posttranslational modifications (PTM), such as phosphorylation, SUMOylation, ubiquitination, acetylation, and O-GlcNAcylation. The understanding of PTMs modulation of PPARs function could contribute for the development of metabolic diseases treatment with more specificity and fewer side effects. Therefore, in this chapter, we present an overview of PTMs that modulate the activity of each PPAR isotype and strategies to modulate these PTMs and thus regulate PPARs action.

7.6. APÊNDICE F – ARTIGO PUBLICADO EM COLABORAÇÃO: EXPLORING THE MOLECULAR PATHWAYS OF THE ACTIVATION PROCESS IN PPARγ RECURRENT BLADDER CANCER MUTANTS

RESEARCH ARTICLE | OCTOBER 23 2024

Exploring the molecular pathways of the activation process in PPARγ recurrent bladder cancer mutants

Vinícius M. de Oliveira; Caique C. Malospirito; Fernando B. da Silva; Natália B. Videira; Marieli M. G. Dias; Murilo N. Sanches; Vitor B. P. Leite; Ana Carolina M. Figueira

+ Author & Article Information

J. Chem. Phys. 161, 165102 (2024)

https://doi.org/10.1063/5.0232041 **Article history**

The intricate involvement of Peroxisome Proliferator-Activated Receptor Gamma (PPARγ) in glucose homeostasis and adipogenesis is well-established. However, its role in cancer, particularly luminal bladder cancer, remains debated. The overexpression and activation of PPARγ are implicated in tumorigenesis. Specific gain-of-function mutations (M280I, I290M, and T475M) within the ligand-binding domain of PPARγ are associated with bladder cancer and receptor activation. The underlying molecular pathways prompted by these mutations remain unclear. We employed a dual-basin structure-based model (db-SBM) to explore the conformational dynamics between the inactive and active states of PPARγ and examined the effects of the M280I, I290M, and T475M mutations. Our findings, consistent with the existing literature, reveal heightened ligand-independent transcriptional activity in the I290M and T475M mutants. Both mutants showed enhanced stabilization of the active state compared to the wild-type receptor, with the I290M mutation promoting a specific transition route, making it a prime candidate for further study. Electrostatic analysis identified residues K303 and E488 as pivotal in the I290M activation cascade. Biophysical assays confirmed that disrupting the K303–E488 interaction reduced the thermal stabilization characteristic of the I290M mutation. Our study demonstrates the predictive capabilities of combining simulation and cheminformatics methods, validated by biochemical experiments, to gain insights into molecular activation mechanisms and identify target residues for protein modulation.

8. ANEXOS

8.1. Autorização da editora para inserção do artigo publicado na tese

Open access

Frontiers' open access policy ensures high visibility and maximum exposure of your work - anyone can read your Frontiers articles, without paying any access or subscription costs. Your work can be shared under the terms of the Creative Commons Attribution License. Frontiers submits all its journals for archiving in PubMed Central and PubMed, and all publications receive a PMCID as soon as the journal is indexed (even retroactively).

Copyright retention

Under our website terms and conditions you retain the copyright in your articles (except for any third-party images etc). You may in general reproduce copies of your articles in any way you choose and freely disseminate these as reprints or electronically, as long as the original publication is fully cited. For instance, your published article can (with the full citation) be posted on your personal or institutional homepage, emailed to friends and colleagues, printed, archived in a collection, distributed on CD-ROM, quoted in the press, translated or distributed in any other way to as many people and as often as you wish. All Frontiers articles are Open Access and distributed under the terms of the Creative Commons Attribution License, which permits the use, distribution, and reproduction in other forums, provided the original authors and source are credited.

https://www.frontiersin.org/journals/endocrinology/for-authors/

8.2. Declaração de direitos autorais

Declaração

As cópias de artigos de minha autoria ou de minha co-autoria, já publicados ou submetidos para publicação em revistas científicas ou anais de congressos sujeitos a arbitragem, que constam da minha Dissertação/Tese de Mestrado/Doutorado, intitulada **Explorando a modulação do PPARγ através da fosforilação da S273**, não infringem os dispositivos da Lei n.° 9.610/98, nem o direito autoral de qualquer editora.

Campinas, 26 de janeiro de 2025

Assinatura : _____

Nome do(a) autor(a): **Marieli Mariano Gonçalves Dias**

RG n.° 000980129

Assinatura : _____

Nome do(a) orientador(a): **Ana Carolina Migliorini Figueira**

RG n.°

8.3. Termo de Bioética e Biossegurança

COORDENADORIA DE PÓS-GRADUAÇÃO
INSTITUTO DE BIOLOGIA
Universidade Estadual de Campinas
Caixa Postal 6109. 13083-970, Campinas, SP, Brasil
Fone (19) 3521-6378. email: cpgib@unicamp.br

DECLARAÇÃO

Em observância ao **§5º do Artigo 1º da Informação CCPG-UNICAMP/001/15**, referente a Bioética e Biossegurança, declaro que o conteúdo de minha , intitulada "**Explorando a modulação do PPARγ através da fosforilação da S273**", desenvolvida no Programa de Pós-Graduação em do Instituto de Biologia da Unicamp, não versa sobre pesquisa envolvendo seres humanos, animais ou temas afetos a Biossegurança.

Assinatura: _____
Nome do(a) aluno(a): **Marieli Mariano Gonçalves Dias**

Assinatura: _____
Nome do(a) orientador(a): **Ana Carolina Migliorini Figueira**

Data:
Campinas, 26 de janeiro de 2025